NASA CR-182283

NASA

PLASMA CONTACTOR RESEARCH - 1988

Prepared for

LEWIS RESEARCH CENTER

NATIONAL AERONAUTICS AND SPACE ADMINISTRATION

Grant NAG 3-776

Annual Report

by

John D. Williams

February 1989

Approved by

Paul J. Wilbur
Department of Mechanical Engineering
Colorado State University
Fort Collins, Colorado 80523

(NASA-CR-182283) SPACE PLASMA CONTRACTOR RESEARCH, 1988 Annual Report, 1 Jan. 1988 - 1 Jan. 1989 (Colorado State Univ.) 61 p
CSCL 20I G3/75

N89-21658
Unclas
0204308

NASA
National Aeronautics and Space Administration

Report Documentation Page

1. Report No.	2. Government Accession No.	3. Recipient's Catalog No.
NASA CR-182283		

4. Title and Subtitle

SPACE PLASMA CONTACTOR RESEARCH - 1988

5. Report Date

Feb. 1989

6. Performing Organization Code

7. Author(s)

John D. Williams
Paul J. Wilbur

8. Performing Organization Report No.

10. Work Unit No.

9. Performing Organization Name and Address

Department of Mechanical Engineering
Colorado State University
Fort Collins, CO 80523

11. Contract or Grant No.

NAG3-776

13. Type of Report and Period Covered

Annual
Jan. 1, 1988-Jan. 1, 1989

12. Sponsoring Agency Name and Address

National Aeronautics and Space Administration
Washington, D.C. 20546

14. Sponsoring Agency Code

15. Supplementary Notes

Grant Monitor - Joseph Kolecki, NASA Lewis Research Center
Cleveland, Ohio 44135

16. Abstract

Results of experiments conducted on hollow cathode-based plasma contactors are reported. Specific tests in which attempts were made to vary plasma conditions in the simulated ionospheric plasma are described. Experimental results showing the effects of contactor flowrate and ion collecting surface size on contactor performance and contactor plasma plume geometry are presented. In addition to this work, one-dimensional solutions to spherical and cylindrical space-charge limited double-sheath problems are developed. A technique is proposed that can be used to apply these solutions to the problem of current flow through elongated double-sheaths that separate two cold plasmas. Two conference papers which describe the essential features of the plasma contacting process and present data that should facilitate calibration of comprehensive numerical models of the plasma contacting process are also a part of this report.

17. Key Words (Suggested by Author(s))	18. Distribution Statement
Hollow Cathode Electrodynamic Tether Plasma Contactor	Unclassified-Unlimited

19. Security Classif. (of this report)	20. Security Classif. (of this page)	21. No of pages	22. Price*
Unclassified	Unclassified	56	

TABLE OF CONTENTS

LIST OF FIGURES

THE BASIC PHYSICS OF THE ELECTRON COLLECTION PROCESS

An experimental study of plasma contacting with an emphasis on the electron collection mode of this process was conducted during the grant period. Results describing variations in plasma property profiles and potential differences that develop between a hollow cathode plasma contactor and a simulated ambient plasma were obtained. The basic physical features of the electron collection process were defined on the basis of these experimental results and the difficulties associated with extrapolating results obtained in the laboratory to predict contactor performance in space were reviewed. Although laboratory results can not be expected to predict contactor performance in space perfectly, the laboratory results constitute an important body of data that can serve to validate detailed numerical models of the contacting process. The need for these models to predict contactor performance in space and to facilitate interpretation of data collected in space was pointed out. The details of this work are presented in the paper entitled "Plasma Contacting--An Enabling Technology" which is included as Appendix A to this report.

NON-IDEAL FEATURES OF THE ELECTRON COLLECTION PROCESS AND PRELIMINARY STUDIES OF THE ELECTRON EMISSION PROCESS

Experimental results were obtained during the grant period which describe operation of and the plasma environment associated with a hollow cathode-based plasma contactor collecting electrons from an ambient, low density Maxwellian plasma when the boundary between the contactor and the ambient plasma is nearly hemispherical. Basic physical features of the process of electron collection identified on the basis of these results were shown to include 1) a double-sheath across which a substantial potential difference can develop and 2) substantial ionization of neutral gas coming from the cathode by the electrons being collected. Experimental results obtained when the diameter of the anode was too small to yield a hemispherical double-sheath were shown to induce distortion of this sheath. It was argued, however, that the same basic phenomena associated with the hemispherical sheath were still active in this case. Data obtained in these experiments should also serve to validate numerical models of this process that are being developed to predict plasma contactor performance in space. Preliminary performance and plasma property results measured on a contactor emitting electrons were examined and some physical elements of this process were identified. A detailed description of this work entitled "Ground-Based Tests of Hollow Cathode-Based Plasma Contactors" was written. It is included as Appendix B to this report.

PLASMA CONTACTOR-RELATED EXPERIMENTS AND DEVELOPMENTS

INTRODUCTION

A plasma contactor is a device that can be used to remove and control electrical charge buildup on satellites by generating a relatively dense plasma that can couple spacecraft surfaces to each other and to the ionospheric plasma. In this particular application a plasma contactor serves essentially the same function as a terestrial grounding wire. In electrodynamic tether applications, on the other hand, plasma contactors serve as electrical "brushes". An electrodynamic tether system consists of two satellites connected by a long, conducting wire. When such a system is gravity gradient stabilized in an equatorial orbit around the Earth the tether will cut across the geomagnetic field lines and a potential difference will be induced between the two satellites. If an electrical load and two plasma contactors (one at each satellite) are connected in series with the tether (and if the plasma contactors are efficient "brushes" which establish an electrical connection between each end of the tether and the stationary ionospheric plasma), current will flow through the tether and electrical power can be converted directly from the orbital energy of the tethered satellite system. In an electrodynamic tether system, plasma contactor performance can have an important influence on the efficiency of power generation and the safety of the mission because of the high currents (ampere levels) and high voltages (about 3000 V for a 20 km tether in LEO) involved.

This report will discuss ground-based tests of plasma contactors. It will concentrate on describing the plasma contacting performance of a hollow cathode plasma source. Specific experiments which address the simulated ionospheric plasma properties will be discussed, along with simple models of the important processes observed. In order to avoid reproduction of the information described in Appendices A and B of this report extensive reference will be made to the material presented there.

APPARATUS AND PROCEDURE

The vacuum chamber used to test the hollow cathode-based plasma contactor is cylindrical with a diameter of 1.2 m and a length of 5.3 m. The contactor was typically placed at one end of the chamber on the centerline, while a second hollow cathode source (the simulator), which was used to produce the simulated ionospheric plasma, was positioned 2.7 m away. The pressure within the vacuum chamber was typically in the range of 3 to 8 $x10^{-6}$ Torr during tests when both the contactor and simulator devices were operated. The hollow cathode devices, mechanical and electrical schematics, and plasma diagnostic instruments are described in Appendices A and B.

The procedure used to test the plasma contactor consisted of first starting the contactor and simulator discharges and setting them to prescribed values. Next, the contactor and its associated plasma were biased with respect to the ambient plasma and the current flow induced at this bias condition was measured. By changing the bias voltage and measuring the corresponding current, a plot which

describes the performance of the contactor can be constructed. At each bias voltage/current condition plasma properties were measured throughout the region between the contactor and simulator. A summary of results obtained during tests are described in Appendix A, while more detailed discussions and results are presented in Appendix B.

In order to study the effects of the simulator on the ambient plasma conditions, its 3 cm diameter, flat plate anode was modified so it could be positioned at distances that ranged from 0 to 10 mm from the simulator cathode. By moving the simulator anode it was determined that some control over the ambient plasma density in the vacuum chamber could be achieved. In another experiment a surface on which ions could be collected was positioned within the contactor plasma plume. This was done so the effects of removing ions from the contactor plume region could be studied.

GENERAL OBSERVATIONS

Many physical phenomena which are observed in ground-based experiments of plasma contactors can be described using a plot of plasma potential versus axial position. A general example of such a plot is shown in Fig. 1. In this figure, the contactor at the left-hand side is collecting electrons (the collector) and the simulator at the right hand side is emitting them (the emitter). The collector double sheath that develops near the collector can sustain potential drops between 10 and 100 V; depending to first order on such variables and parameters as the electron current being collected, the contactor flowrate and the contactor anode size. The small potential dip

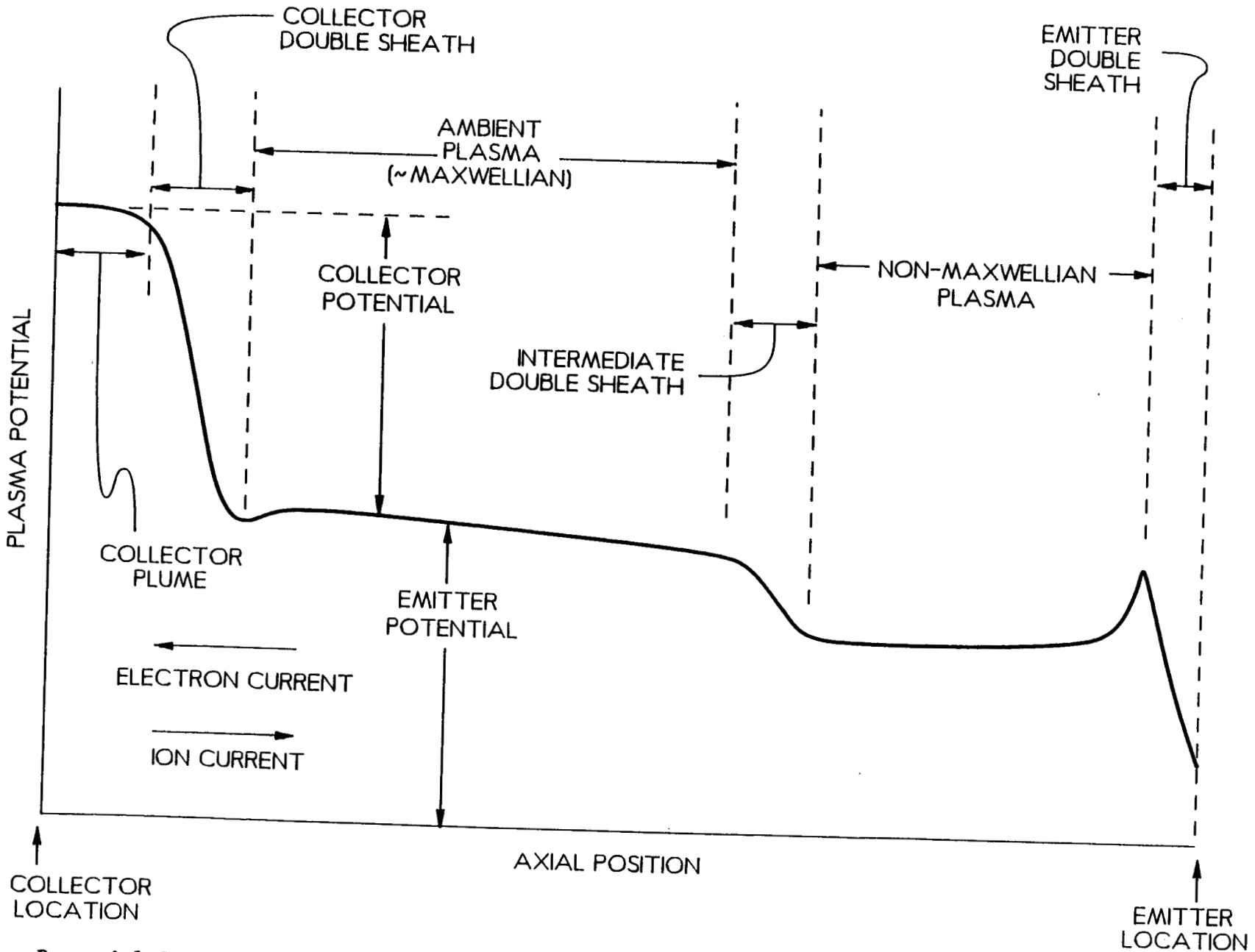

Fig. 1. Potential Structure between Contactors Emitting and Collecting Electrons

separating the ambient plasma and the collector double sheath has been observed in most experiments. Such dips have been observed and modelled by other researchers.[1] Their results suggest that this dip occurs (and the electron and ion currents counterflowing through the double-sheath are also enhanced) because the ambient plasma Maxwellian electron population have a non-zero temperature (T_{eo} ~ 5 to 7 eV) and they therefore approach the sheath with non-zero velocities. It is noted that the ambient plasma electron population typically consists of a Maxwellian electron group (comprising about 95% of the total electron density) and a second mono-energetic or primary electron group (which normally exhibits an energy of ~ 30 to 80 eV) which contributes the remaining density. Consequently, most of the electrons flowing through the double-sheath are electrons that are drawn from the ambient plasma Maxwellian group. Analysis suggests the ambient plasma density is sustained principally by volume ionization of neutral atoms that are present in the vacuum tank. This ionization is induced by both Maxwellian and mono-energetic electrons at rates that are of the same order under most experimental conditions.

The paper in Appendix B shows that the product of the surface area of the downstream boundary of the collector double sheath and the random current density of the ambient plasma is equal to the electron current being drawn from the ambient plasma through the collector double sheath into the collector plume. In addition, this paper shows that the ion current emitted from the collector plasma plume is proportional to the electron current and the square root of the electron/xenon ion mass ratio. This experimental result, along with calculations indicating that very few elastic and inelastic collisions

occur within the collector double-sheath, confirm earlier assumptions that this sheath is doubly space-charge limited and collisionless.

Mono-energetic electrons have been observed streaming from the collector double-sheath toward the contactor in the collector plume shown in Fig. 1. These electrons presumably comprise a beam, however, no measurements of turbulence have been made in this region to determine if streaming instabilities develop there. In Appendices A and B simple models have been used to calculate the ion production rate (due to classical ionizing collisions) in the collector plume region. These calculations show that sufficient ion production occurs there to supply the ions that counterflows against the electrons and assure ion flow is at its space-charge-limited value. Presently, the mechanism by which the collector double sheath is held in a fixed, stable position is uncertain although it does appear that one boundary of the sheath remains tied to the collector anode. It is believed that a collector double sheath will also develop during space tests, but whether or not it will be stable and well-defined is uncertain. Questions concerning the development of double sheaths are considered to be of primary importance, because ground-based tests have shown that the dominant voltage drop associated with collector operation occurs at double sheaths and their existance would therefore be expected to exert a significant influence on the electrodynamic tether system efficiency.

The intermediate double sheath shown in Fig. 1, which forms downstream of the ambient plasma region, is typically located ~100 to 200 cm from the contactor emitting electrons (the emitter) and a potential drop of ~10 V generally develops across it. Presently it is

believed that the intermediate double sheath is caused by interactions between the vacuum chamber wall and the plasma being produced near the emitter. It is appears that this sheath separates a beam-dominated, low-density plasma region which surrounds the emitter from the ambient plasma. This non-Maxwellian, beam-dominated plasma region is shown in Appendix B to contain a electrons that are expanding in a spherical fashion from the point at which the emitter is located. The potential hump immediately adjacent to the emitter double sheath appears to develop because electrons being drawn from the emitter induce ionization of the neutral atoms in this region at a high rate. The potential drop across the emitter double sheath has been observed to range from 20 to 80 V depending upon the emitter operating conditions.

Effects of Simulator Operating Conditions

A simplified plasma potential profile that doesn't contain the detailed structure of Fig. 1 is shown in Fig. 2. When experiments are being conducted and the contactor at the origin of the potential plot is collecting electrons as it is in this case, it is this collector that is being investigated. The other plasma source, which is not located at the origin where instruments are available to probe it, serves to generate the ambient plasma from which electrons can be collected for the experiment. This source is designated the "simulator". Also shown in Fig. 2 is a sketch of the simulator hollow cathode device showing its flat plate anode which can be moved during operation to change the cathode/anode separation distance X_a. Terms defined on the plasma potential profile shown in Fig. 2 are the potential difference between the ambient plasma and the simulator cathode, labeled ΔV_S and the potential difference between the

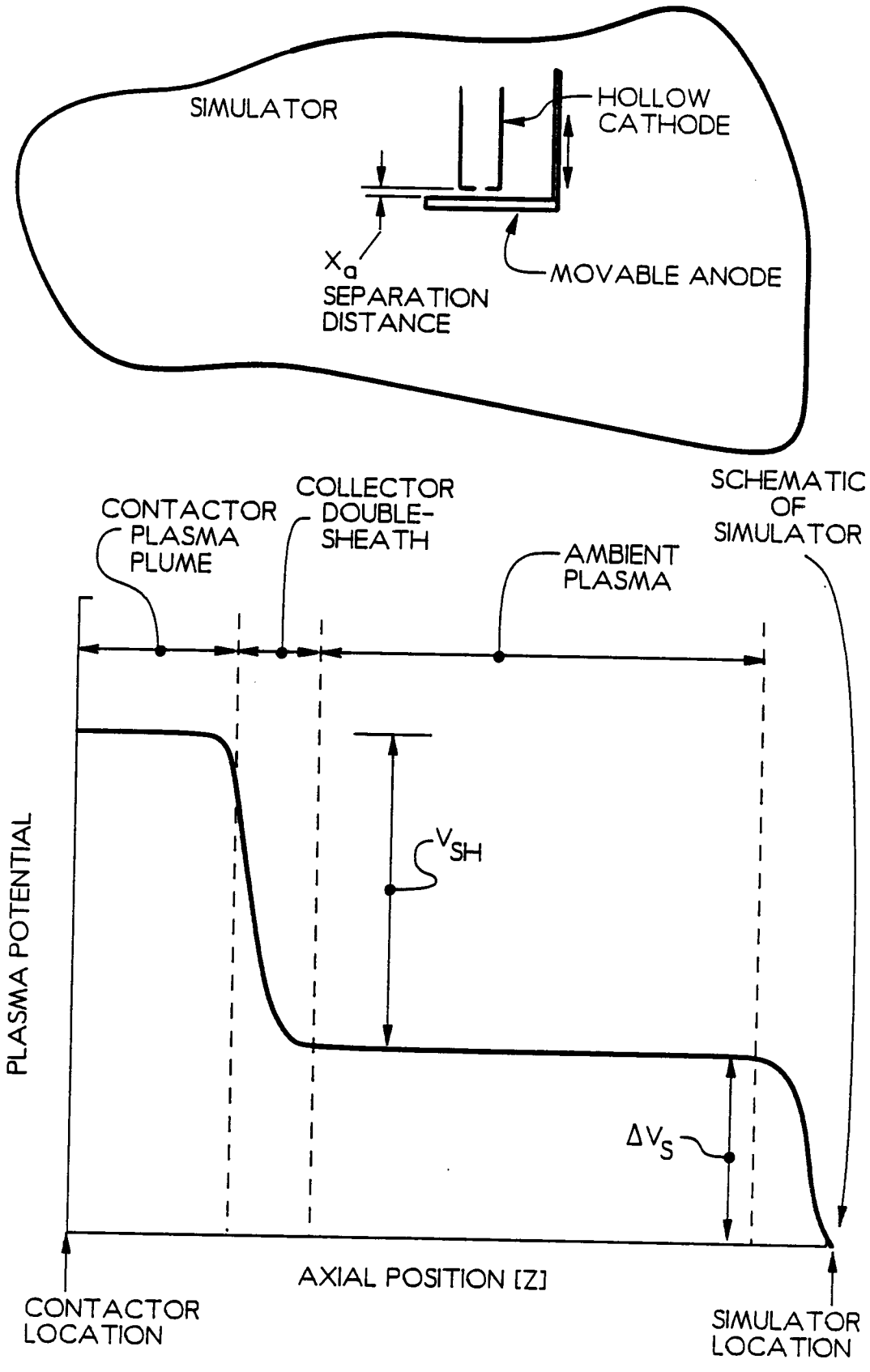

Fig. 2. Simplified Potential Structure at Collector

contactor anode and the ambient plasma, labeled V_{SH}. Note that the potential drops associated with the emitter, the emitter double sheath and the intermediate double sheath are all lumped together and designated by the voltage drop ΔV_S.

In order to study the effects of simulator operating and design parameters on the ambient plasma properties, the following experiment was performed. First, the simulator and collector flowrates were set at 2 and 3.4 standard cubic centimeters per minute of xenon (sccm (Xe)). This induced a vacuum chamber background pressure of 3.5×10^{-6} Torr. Next, the collector and the collector plasma plume were biased positive with respect to the ambient plasma and the electron collection current (J_{CE}) and ambient plasma properties were measured. This procedure was repeated for several different collector bias conditions. A typical plot of ambient plasma density versus contactor electron collection current measured in this test is shown in Fig. 3. This figure shows that the ambient plasma density varies linearly with electron collection current when the tests are carried out in a ground-based vacuum tank as they were in this case. The ambient plasma potential measured during the experiment corresponding to Fig. 3 remained at about 40 to 50 V (from Fig. 2 this means that ΔV_S also remained at about 40 to 50 V). Consequently, Fig. 3 suggests that the ionization rate occurring within the ambient plasma, which controls the plasma density in this region, is proportional to the simulator electron emission current. It is noted that the electron current emitted by the simulator agreed with the current collected by the contactor to within 1% in this case and for all other data presented in this report unless specifically stated otherwise.

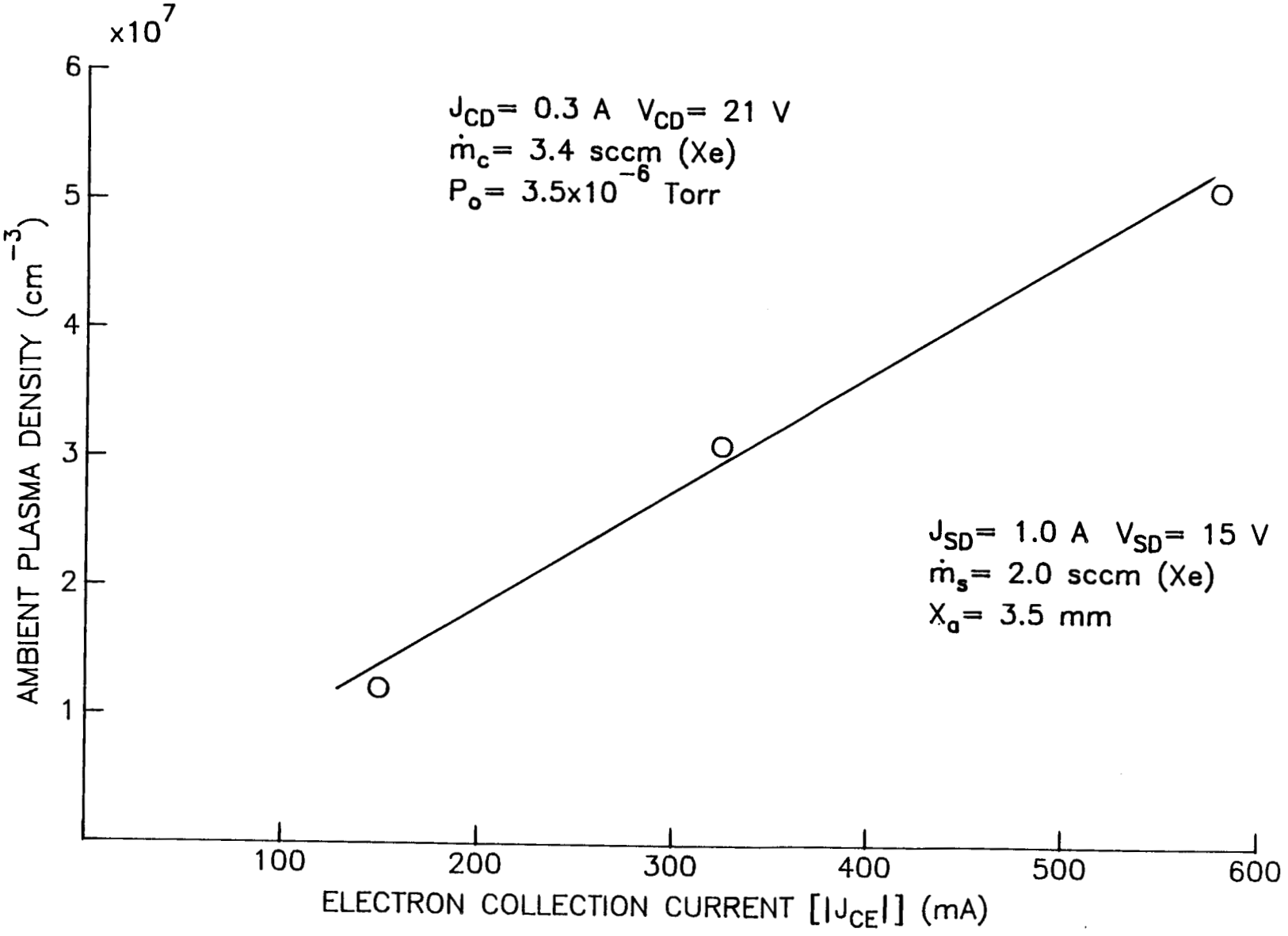

Fig. 3. Typical Effect of Electron Collection Current on Ambient Plasma Density

Finally, it is noted that the variation of ambient plasma density with electron collection current observed in these ground-based tests would not be expected in a space test. There, the large reservoir of ambient plasma should be essentially unaffected by changes in collection current.

Calculations of the ion production rate induced by electrons emitted from the simulator suggest that the ambient plasma density should also depend on the energy at which these electrons enter the ambient plasma. In order to test this hypothesis, the parameter ΔV_S was varied by changing the simulator anode/cathode separation distance X_a while the contactor electron collection current was held constant. As shown by the data contained in Fig. 4, the ambient plasma density is indeed dependent upon ΔV_S, and in fact it can be changed by a factor of four by reducing X_a from 3.5 to 1 mm. The size of the collector double-sheath region was also observed to shrink at a given electron current condition when the ambient plasma density was increased. Reductions in X_a below ~1 mm induced continued increases in ΔV_S, but they these lower values of the simulator anode separation distance were not investigated because large noise-to-signal ratios were observed on Langmuir probe traces collected under these conditions; this noise made analysis of the Langmuir probe traces impossible. The noise was observed to correlate with oscillations of the collector plume boundary. The frequency of oscillation was typically between one and ten Hertz, but lower amplitude, higher frequency oscillations could have also been present. No measuremments of the frequency spectra associated with this noise were made.

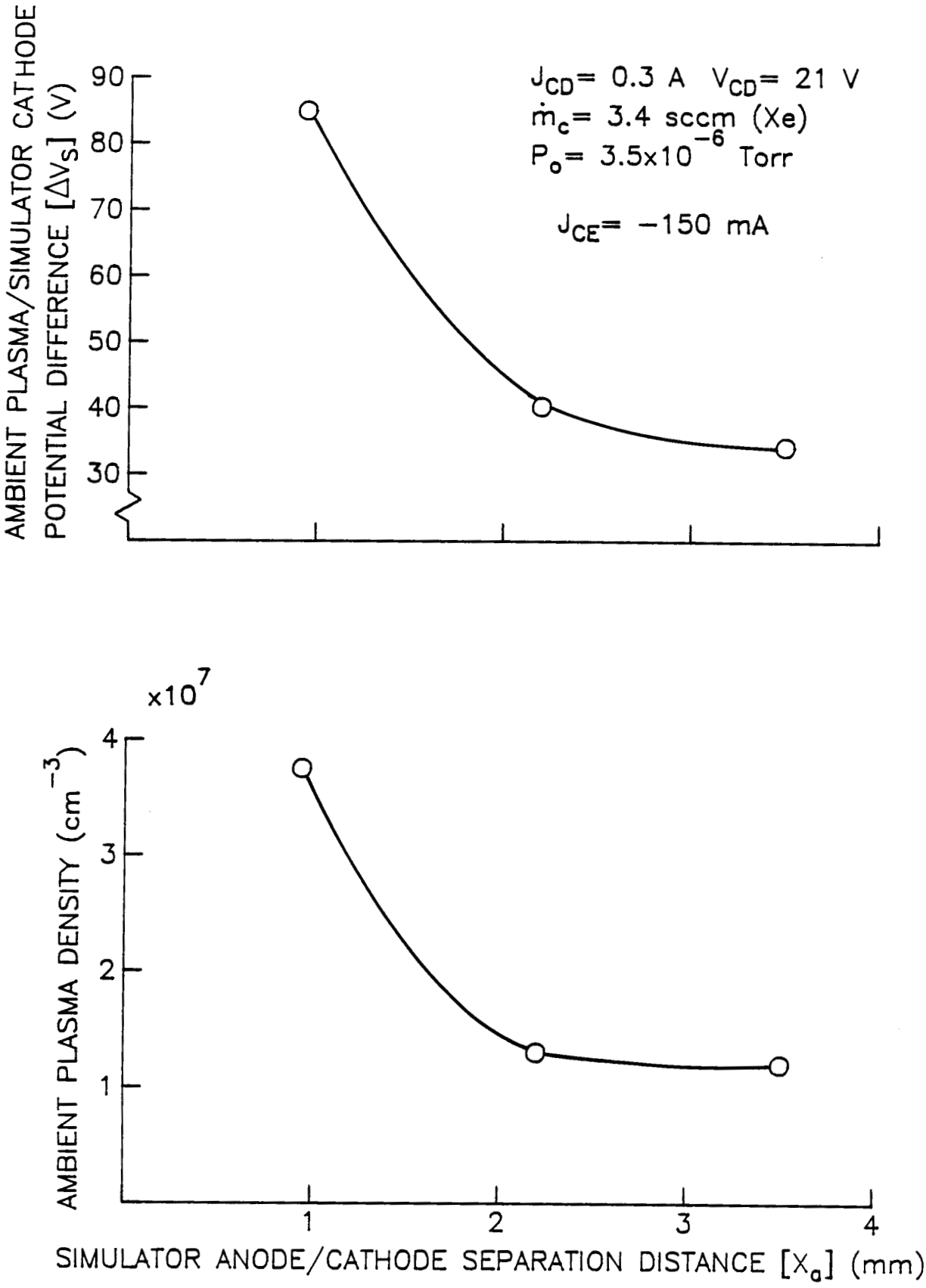

Fig. 4. Effect of Simulator Anode/Cathode Separation on Ambient Plasma

In another test, the simulator discharge current was changed in order to vary ΔV_S and the results of this test are shown in Fig. 5. Again increasing ΔV_S caused the ambient plasma density to increase under the prescribed constraint of operation at a constant electron collection current. It is noted that the electron temperature within the ambient plasma was nearly constant at ~6 to 7 eV over the complete range of plasma densities associated with the data in Figs. 3, 4 and 5; and this temperature along with the ambient Maxwellian electron density generally indicated ion production rates comparable to ion production rates caused by mono-energetic electrons being supplied by the simulator.

A possible explaination for the increase in ΔV_S that accompanies reductions in simulator discharge current and/or anode/cathode separation distance is considered to be related to changes in plasma density in the region immediately adjacent to the simulator. Both low discharge currents and small anode/cathode spacings (which would enhance ion recombination) could cause the plasma in this region to have a low density. These lower plasma densities would in turn be expected to necessitate larger potential differences between the simulator and the ambient plasma to extract a given electron emission current.

Cylindrical and Spherical Space-Charge Limited Double-Sheath Analysis

A first-order approximation of the potential drop across a collector double sheath and an understanding of the basic processes occurring in this region can be obtained by solving the cylindrical and spherical space-charge-limited double-sheath problems. The solution to the spherical double sheath is given in Ref. 1. The

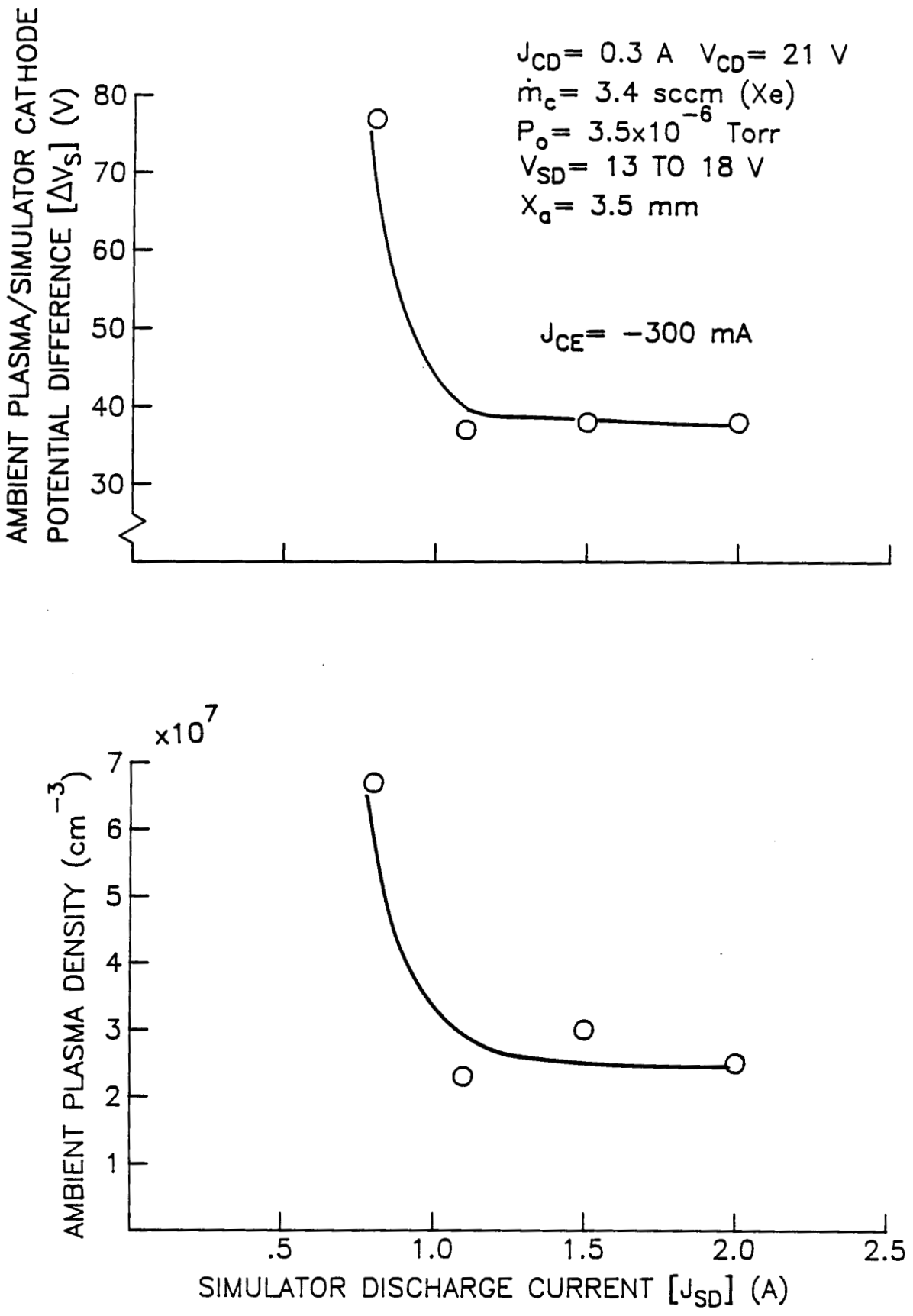

Fig. 5. Effect of Simulator Discharge Current on Ambient Plasma

equations and boundary conditions used to obtain that solution will be summarized here along with similar equations and boundary conditions needed to solve the cylindrical double-sheath problem. The schematic shown in Fig. 6 suggests a possible shape for a double-sheath region which might be modeled using a combination of spherical and cylindrical segments. This shape is similar to the experimentally measured shapes shown in Fig. 6 of Appendix A and Figs. 6 and 13 of Appendix B. The spherical and cylindrical segments of the double-sheath region shown in Fig. 6 can be modeled using the equations[2] listed as items 1, 2 and 3 in Table 1. Solving these equations numerically for values of j_o (the normalized current from the outer surface[2]) and α versus double-sheath radius ratio ($r_{i_{cyl}} / r_{o_{cyl}}$ and $r_{i_{sph}} / r_{o_{sph}}$) for the boundary conditions cited under item 6 in Table 1 allows one to construct the plots shown in Figs. 7 and 8. The equations given as item 4 in Table 1 and the corresponding plots of Figs. 7 and 8 can be applied to predict the voltage drop across the double sheath once the double-sheath dimensions have been determined. These dimensions can be calculated using the procedures discussed in Ref. 3.

Although, the model inherent in the expressions of Table 1 and the numerical results of Figs. 7 and 8 appear to be valid when the ratio of electron collection current-to-contactor anode diameter is small, it generally yields voltage drops that are larger than those measured experimentally when this condition is not met. Specifically, the voltage drops measured experimentally from plasma potential profiles corresponding to large electron collection

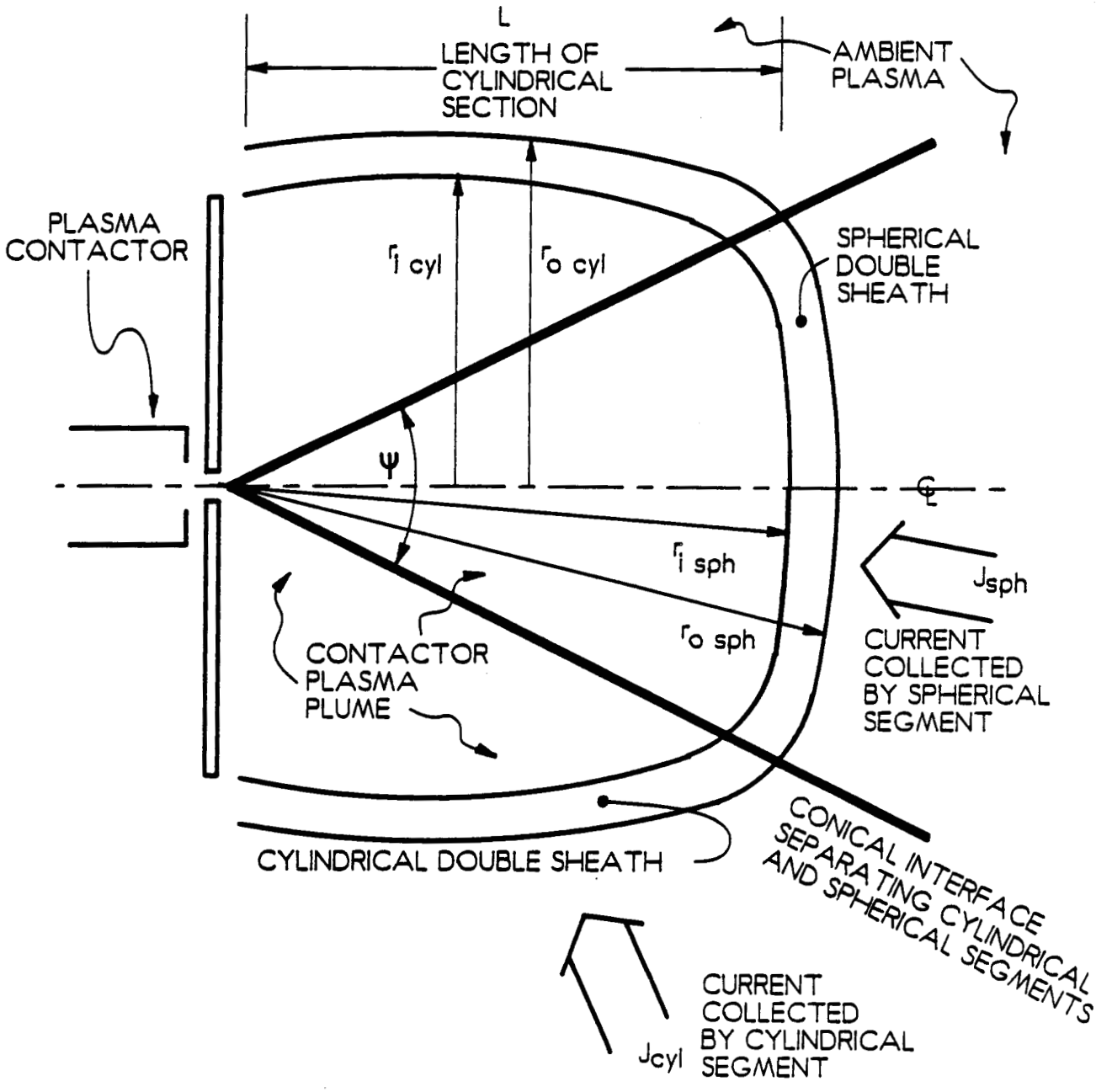

Fig. 6. Schematic of Cylindrical/Spherical Double-Sheath

TABLE 1. Cylindrical and Spherical Double-Sheath Space-Charge Limited Analysis

Cylindrical Equations:	Spherical Equations:
1. $\nabla^2 V = -\frac{e}{\epsilon_0}(n_+ - n_e)$	1. same
2. $J_{+_{cyl}} = e\, n_+\, 2\pi r L \sqrt{\frac{2e(V_i - V)}{m_+}}$	2. $J_{+_{sph}} = e\, n_+\, \psi\, r^2 \sqrt{\frac{2e(V_i - V)}{m_+}}$
3. $J_{cyl} = e\, n_e\, 2\pi r L \sqrt{\frac{2eV}{m_e}}$	3. $J_{sph} = e\, n_e\, \psi\, r^2 \sqrt{\frac{2eV}{m_e}}$
4. Non-Dimensional Definitions	
a. $\phi = \frac{V}{V_i}$	a. same
b. $\rho = \frac{r}{r_0}$	b. same
c. $j_0 = \frac{J_{cyl}\frac{r_0}{L}}{2\pi\epsilon_0\sqrt{\frac{2e}{m_e}}\, V_i^{3/2}}$	c. $j_0 = \frac{J_{sph}}{\psi\,\epsilon_0\sqrt{\frac{2e}{m_e}}\, V_i^{3/2}}$
d. $\alpha = \frac{1}{1 + \frac{1}{4j_0}\int_{\rho_i}^{1}\left[\frac{d\phi}{d\rho}\right]^2 d\rho} = \frac{J_{cyl}}{J_{+_{cyl}}}\sqrt{\frac{m_e}{m_+}}$	d. $\alpha = \frac{1}{1 + \frac{1}{2j_0}\int_{\rho_i}^{1}\left[\frac{d\phi}{d\rho}\right]^2 d\rho} = \frac{J_{sph}}{J_{+_{sph}}}\sqrt{\frac{m_e}{m_+}}$
5. Non-Dimensional Governing Equation	5.
$\rho\frac{d^2\phi}{d\rho^2} + \frac{d\phi}{d\rho} = j_0\left[\frac{1}{\sqrt{\phi}} - \frac{1}{\alpha\sqrt{1-\phi}}\right]$	$\rho^2\frac{d^2\phi}{d\rho^2} + 2\rho\frac{d\phi}{d\rho} = j_0\left[\frac{1}{\sqrt{\phi}} - \frac{1}{\alpha\sqrt{1-\phi}}\right]$
6. Boundary and Space-Charge Limited Conditions:	
a. $\phi(\rho_i) = 1$	a. same
b. $\phi(1) = 0$	b. same
c. $\frac{d\phi}{d\rho} = 0$ at $\rho=\rho_i$ and $\rho=1$	c. same

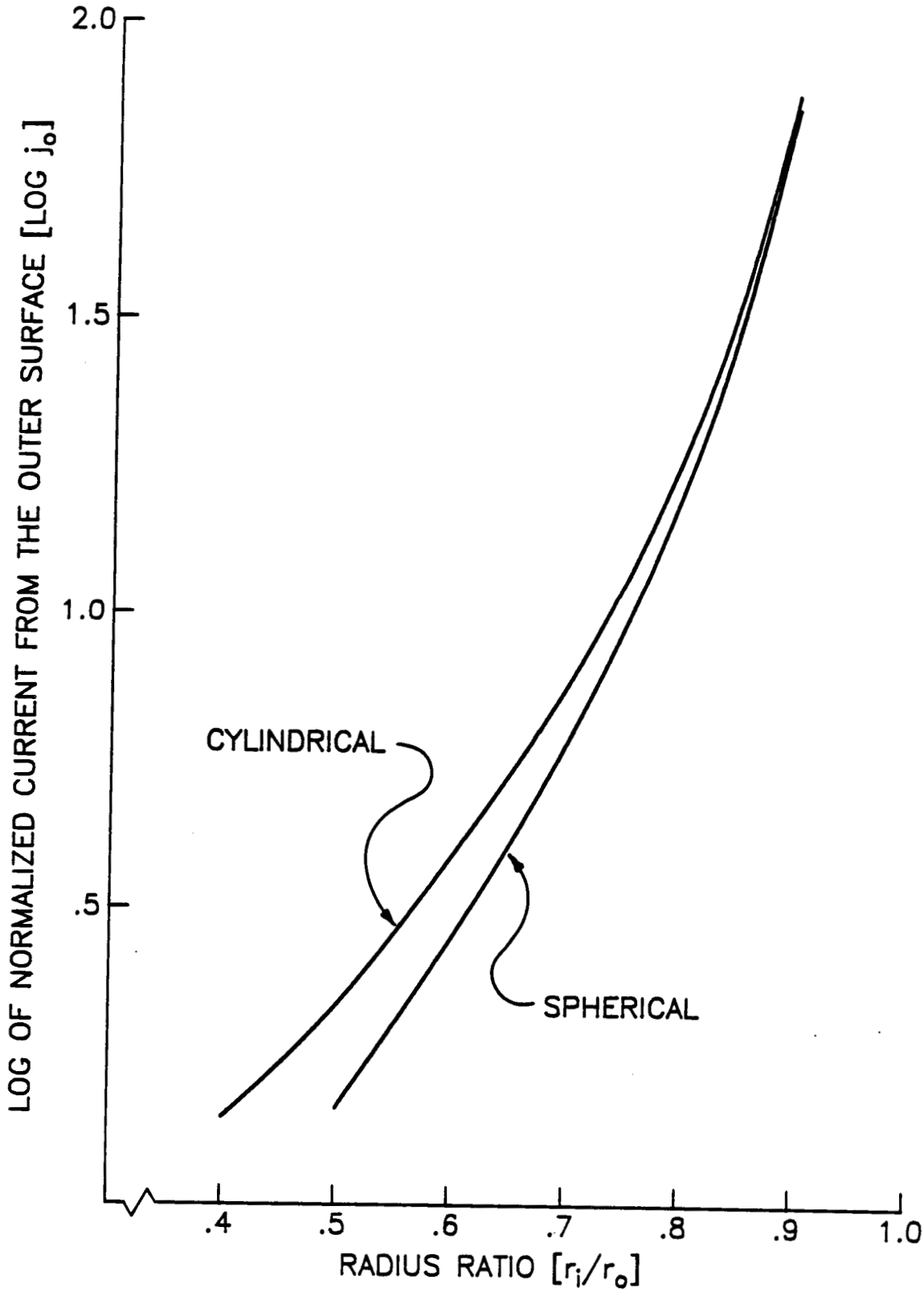

Fig. 7. Effect of Radius Ratio on Parameter j_o

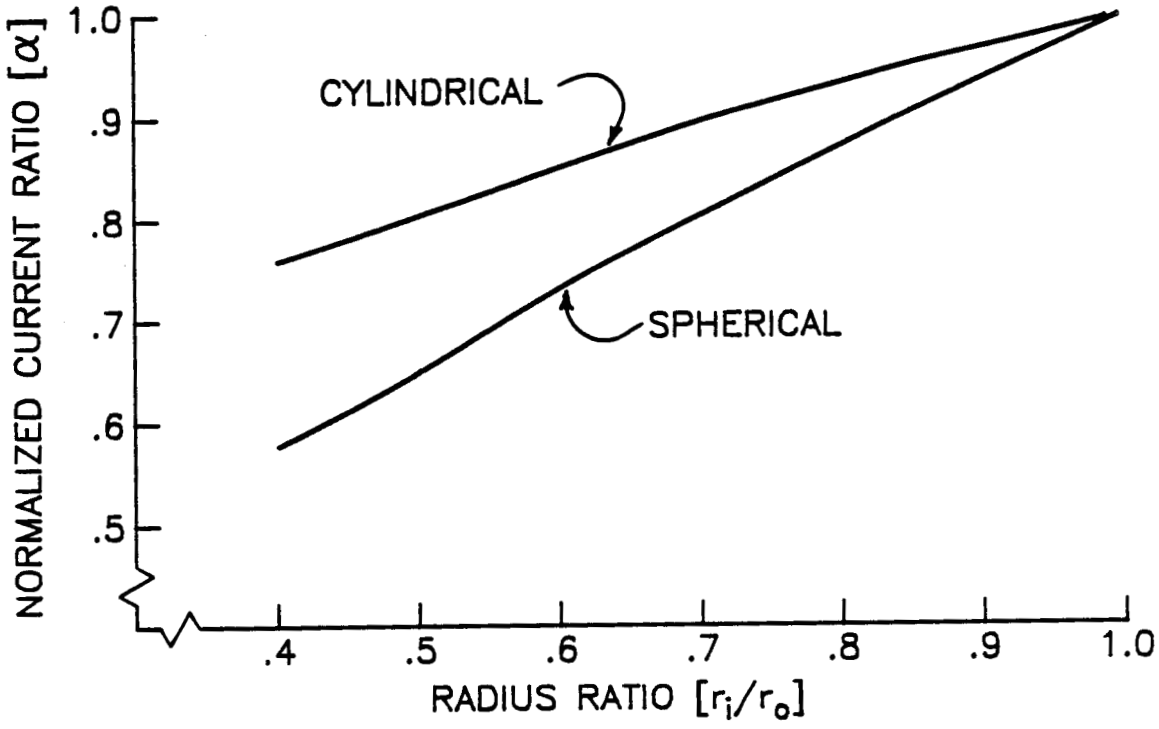

Fig. 8. Effect of Radius Ratio on Parameter α

currents[4] and small anode diameters (also see Appendix B) and contactors operating in the electron emission mode (see Appendices A and B) are smaller than those predicted to the model. In all of these cases, the experimentally measured inner boundary of the double sheath becomes less pronounced, the ratio of the inner/outer double-sheath dimensions increases and this means the sheath thickness increases. Contrary to experimental results obtained during these tests, the model inherent in Table 1 indicates that an increasing sheath thickness should induce an increase in the sheath potential drop. It is expected that models suggested by theoretical researchers[5] which can include the effects of non-radial trajectories of the electrons being collected and ionization in the sheath will provide an explanation for the breakdown of the simple double-sheath proposed here under these conditions.

Effects of Ion Collecting Surfaces Placed within the Contactor Plasma Plume

In order to determine if the observed deviations from the simple double-sheath model observed in experiments involving high electron collection currents and/or small anode diameters were caused by different ion production/loss mechanisms, an experiment was conducted in which a relatively large (5 cm diameter), electrically floating, screened plate was placed within a typical, well-defined collector plasma plume region. It was believed that the surface would remove ions from the collector plasma plume at a rate which would significantly distort the plasma plume geometry. The experiment was conducted when the contactor was collecting 600 mA from the ambient plasma. The results obtained from the test are presented in Fig. 9 in

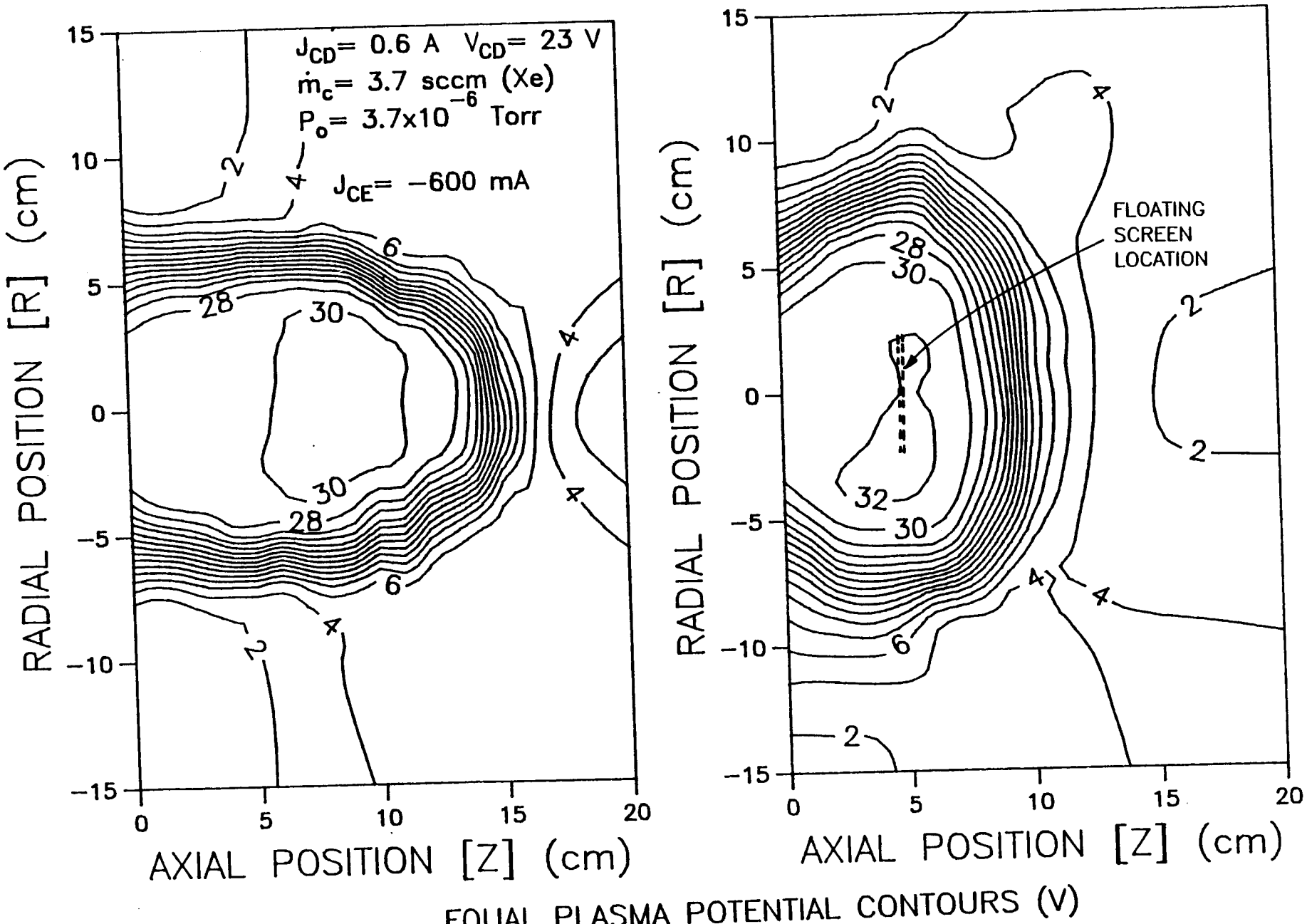

Fig. 9. Effects of an Ion Collecting Surface Placed within Contactor Plume

the form of two comparative equipotential contour maps (one with the screen installed ~5 cm downstream of the collector anode and one with no screen). The plasma potentials shown in this figure are referenced to the ambient plasma potential, which was ~ 45 V in both cases. Comparison of Figs. 9a and 9b shows that placement of the 5 cm diameter plate parallel to and concentric with the anode does modify the shape of the contactor plasma plume. However, instead of causing it to collapse radially inward toward the collector cathode, it caused the plume to expand radially. It is noted that the ambient plasma conditions for Figs. 9a and 9b were nearly identical (specifically, the plasma density was 2 x 10^7 cm^{-3} and the electron temperature was 7.0 eV). Although placing the 5 cm diameter plate in (and presumably removing ions from) the plume altered its geometry no conclusive data was obtained which proved that the geometrical changes observed when one reduces the anode diameter or the increases electron collection current are related to changes in the rate of ion production or loss rates occurring within the collector plasma plume.

Effects of Flowrate on Double-Sheath Geometry

In addition to anode size and electron collection current, contactor flowrate (and indirectly system background pressure) can also influence the geometry of the contactor plasma plume and the double sheath. In order to demonstrate the effects of flowrate on the sizes and geometries of the double sheath and collector plume, an experiment was conducted in which collector flowrate was varied, potential profile data were collected and Fig. 10 was constructed. It shows four equipotential contour plots corresponding to contactor flowrates of 2.7, 4.1, 7.0 and 11 sccm (Xe). Note that the

J_{CD}= 0.3 A, V_{CD}= 11 TO 20 V, J_{CE}= −900 mA

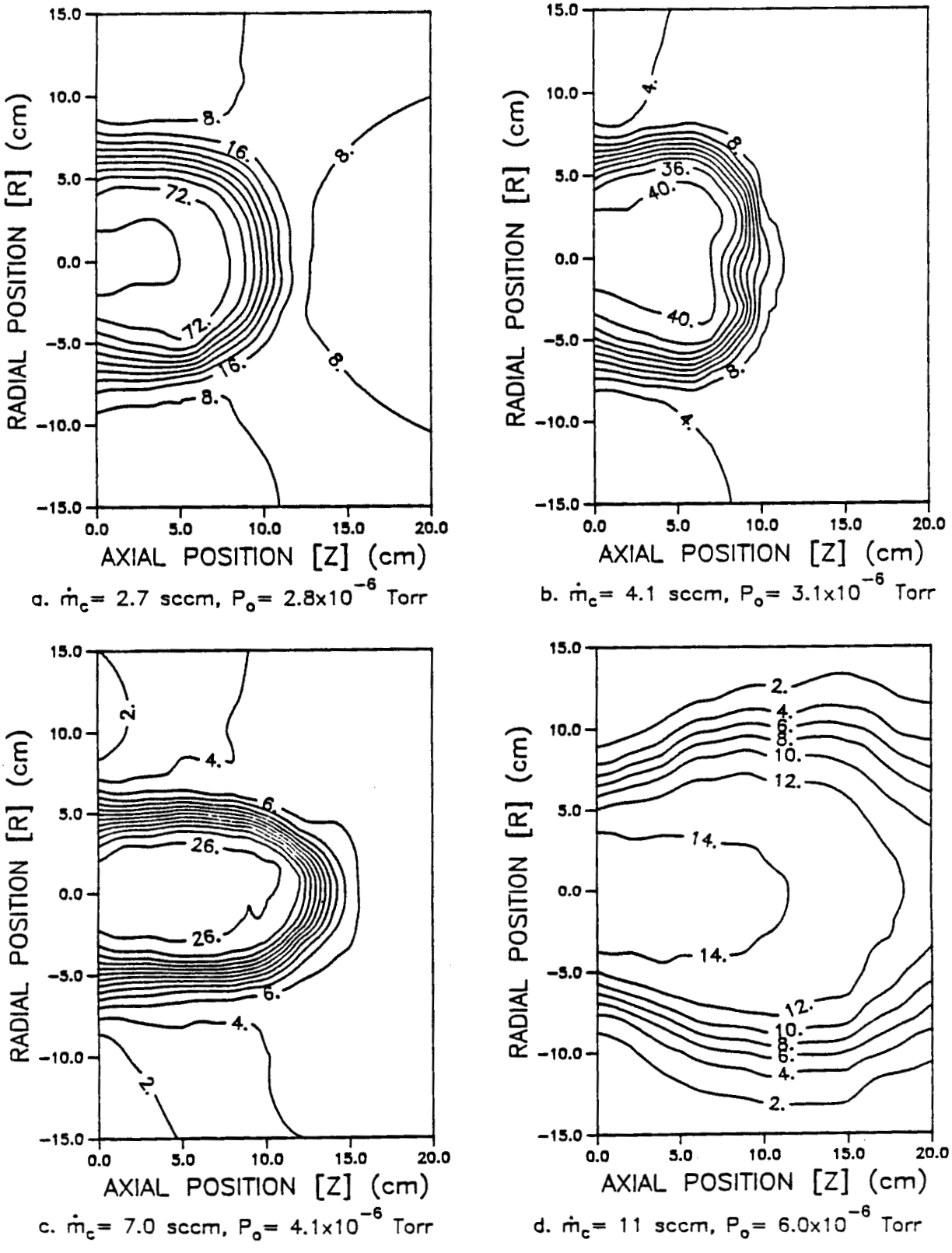

a. $\dot{m}_c$= 2.7 sccm, P_o= 2.8x10^{-6} Torr

b. $\dot{m}_c$= 4.1 sccm, P_o= 3.1x10^{-6} Torr

c. $\dot{m}_c$= 7.0 sccm, P_o= 4.1x10^{-6} Torr

d. $\dot{m}_c$= 11 sccm, P_o= 6.0x10^{-6} Torr

Fig. 10. Effects of Flowrate on Plasma Potential Field

equipotential contours are measured with respect to the ambient plasma potential. The lowest flowrate required a large sheath potential drop (72 V) in order to collect the 1 A of electron current. This large sheath potential drop is required in order to produce the ion current which counterflows through the space-charge limited region since fewer neutral atoms are present at this flowrate condition (see Appendix B). As the flowrate is increased to progressively higher values, lower sheath potential drops are observed and the geometry of the double sheath changes. Both the geometrical and sheath potential differences observed between the four flowrate conditions are believed to be induced by changes in the locations at which ion production and loss occurs and by the fact that one double-sheath boundary remains tied to the anode.

CONCLUSIONS

The potential difference that develops between an ambient plasma and a simulator and the magnitude of the electron current being emitted at the simulator exhibits a strong influence on the ambient plasma density in ground-based tests. Ambient plasma density can be controlled to some extent by contolling this potential difference, but noise is encountered if the ambient plasma density becomes too great.

Simple first-order cylindrical and spherical double-sheath models have been developed and they can be used to predict the potentials and dimensions associated with a double sheath, unless the ratio of electron collection current-to-anode diameter becomes too large. This

double-sheath model does not appear to apply directly to the electron emission process as suggested in Appendix B.

Both collector flowrate and the presence of surfaces on which ions could recombine can effect the geometry of a double sheath. These results suggest that ionization occurring within a collector plume influcence the shape and potential drop associated with a collector double sheath.

REFERENCES

1. Langmuir, I. and K. Compton, "Electrical Discharges in Gases: Part II - Fundamental Phenomena in Electrical Discharges," Reviews of Modern Physics, Vol. 3., No. 2, April 1931.

2. Wei, R. and P.J. Wilbur, "Space-Charge-Limited Current Flow in a Spherical Double Sheath," J. Appl. Phys., Vol. 60, 1 Oct. 1988, pp. 2280-2284.

3. Williams, J.D., P.J. Wilbur, J.M. Monheiser, "Experimental Validation of a Phenomenological Model of the Plasma Contacting Process," appears in "Space Tethers for Science in the Space Station Era," L. Guerriero and I. Bekey, Eds., Societa Italiana D. Fisica, Vol. 14, Venice, Italy, 4-8 Oct. 1987, pp. 245-253.

4. Patterson, M.J. and R.S. Aadland, "Ground-Based Plasma Contactor Characterization," appears in "Space Tethers for Science in the Space Station Era," L. Guerriero and I. Bekey, Eds., Societa Italiana D. Fisica, Vol. 14, Venice, Italy, 4-8 Oct. 1987, pp. 261-268.

5. Katz, I. and V. A. Davis, "Theoretical Developments to Support an Electrodynamic Tether Flight Program Development," Third International Conference on Tethers in Space, San Francisco, May 16, 1989.

Appendix A

AIAA-89-0677
Plasma Contacting - An Enabling Technology

J.D. Williams and P.J. Wilbur
Colorado State University
Fort Collins, Colorado

27th Aerospace Sciences Meeting
January 9-12, 1989/Reno, Nevada

PLASMA CONTACTING--AN ENABLING TECHNOLOGY*

John D. Williams+ and Paul J. Wilbur**

Department of Mechanical Engineering
Colorado State University
Fort Collins, Colorado 80523

Abstract

An experimental study of plasma contacting with an emphasis on the electron collection mode of this process is described. Results illustrating variations in plasma property profiles and potential differences that develop at hollow cathode plasma contactors are presented. A model of the electron collection plasma contacting process that is consistent with experimentally measured results is reviewed. The shortcomings of laboratory results as direct predictors of contactor performance in space and their usefulness in validating numerical models of the contacting process, that can be used to predict such performance, are discussed.

Introduction

Objects placed in a space plasma collect and emit charged particles and they can as a result accumulate net electrical charge. Because the capacitance of a typical spacecraft surface is small, this net charge accumulation can cause the potential of such surfaces to change rapidly and dramatically. A space plasma contactor serves to prevent this problem by providing low impedance electrical connections between spacecraft surfaces and space plasma thereby preventing gross spacecraft charging[1] and between spacecraft surfaces that are isolated from each other thereby preventing differential charging.[2] It can also serve to establish a firm reference potential (local space plasma potential) so the effects of the bias on an instrument can be reflected in the analysis of the data it collects.

In all of these applications the contactor enables the achievement of mission objectives by preventing detrimental charging effects. They are, however, applications in which the contactor is required to handle currents that are typically small and it can conduct them without substantial voltage differences developing. On the other hand, plasma contactors can be used as active elements in such circuits as those associated with electrodynamic tethers[3] where large currents must be conducted and larger voltage differences are expected. On the basis that a contactor that would perform well at high current levels would generally be suitable for use in less demanding applications, this paper will focus on contactors suitable for use in high current (electrodynamic tether) applications.

Typically an electrodynamic tether system includes two spacecraft connected by a long conductive wire or tether in the manner suggested in Fig. 1. When oriented properly, the tether will cut across geomagnetic field lines as it moves in orbit and as a result a voltage difference will be induced between its two ends. In order to take advantage of this voltage difference to generate direct current power, a return path for the current

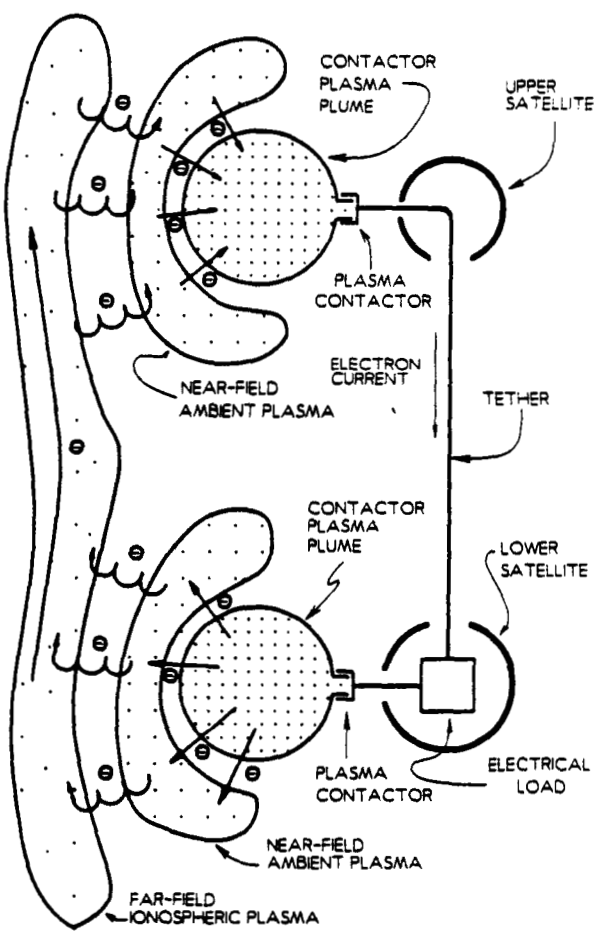

Fig. 1. Conceptualized Electrodynamic Tether Circuit

*Work supported by NASA Lewis Research Center under Grant NAG3-776.

+Research Assistant, Department of Mechanical Engineering.

**Professor, Department of Mechanical Engineering, Member AIAA.

that could flow through the tether and an electrical load must be provided. Figure 1 illustrates a scheme proposed to provide this return path through the ionosphere via plasma plumes that serve as electrical brushes or ionospheric plasma contactors. As the figure suggests, it is desirable to separate this overall contacting process into near and far-field processes. The near-field process is assumed to reflect effects associated with current conduction between adjacent, static plasmas. The far-field process, on the other hand, is assumed to reflect effects associated with relative motion between two plasmas, which are exchanging current, as well as current flow through the geo-scale plasma.

An electrodynamic tether will generate power efficiently provided the load impedance is large compared to the sum of the impedances associated with the tether, the ionosphere and the two contactors shown (one collecting electrons and the other emitting them). Hence, an important characteristic of a plasma contactor is that is exhibit a low voltage drop to ambient plasma at typical operational current levels. Electrons are identified as the principal carriers of this current in Fig. 1 (because they are less massive and therefore more mobile than ions), but it should be recognized that ions are also present and they flow in a direction generally opposite to that of the electrons. Although the ions do not conduct substantial current, it will be shown that they play an important role in determining the contactor-to-ambient plasma potential difference and it is therefore important to remember that they are present.

Hollow Cathode Devices

A review of the desirable characteristics of a plasma contactor (e.g. reliability, simplicity, low expellant and power demands as well as low impedance coupling capability) has suggested that a hollow cathode discharge represents an attractive contactor compared to other alternatives.[4,5] Key features of a hollow cathode and the mechanisms by which it produces a discharge are illustrated in Fig. 2. It consists of a small diameter (of order 1 cm) refractory metal tube that is electron-beam welded to a thoriated tungsten orifice plate. Located within and electrically connected to the tube is a low work function insert from which electrons are emitted. An anode, biased positive of the hollow cathode and located immediately downstream of it, collects a fraction of the electrons being drawn through the cathode orifice. The remaining fraction can be drawn into plasma plumes like those shown in Fig. 1.

The hollow cathode discharge is generally initiated by flowing an expellant gas such as xenon through the cathode tube and orifice, applying power to the heater to raise the insert temperature to thermionic emission levels and applying a bias on the anode that can range, depending on insert temperature, from a few hundred to several thousand volts. Once the insert begins to emit electrons a dense plasma is formed within the cathode and a discharge is established between this plasma and the anode through the orifice. A detailed study of a hollow cathode has suggested[6] that the following physical processes, inferred by the particle motions in Fig. 2, are active:

1. Primary electrons emitted from the insert surface via a field-enhanced thermionic emission process are accelerated into the cathode interior plasma through a sheath at the insert surface.

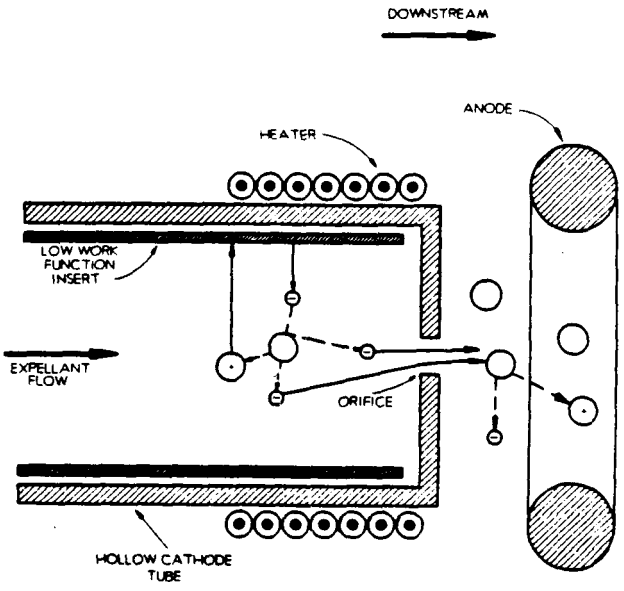

Fig. 2. Hollow Cathode Phenomenological Schematic

2. These electrons acquire sufficient energy as they pass through the sheath so they can ionized neutral atoms present in the hollow cathode interior through multistep, inelastic collision processes.

3. Neither electrons that originate at the insert surface nor those resulting from ionization can reach the insert surface because of the adverse potential gradient that exists in the sheath between the cathode interior plasma and the insert surface. Consequently, they must leave the cathode interior plasma through the orifice at a rate equal to their supply rate.

4. Ions created within the cathode, on the other hand, generally will not go through the orifice because of the adverse potential they see between the cathode interior plasma and the plasma downstream of the orifice. They instead bombard cathode interior surfaces heating them and, in the case of the insert, helping to maintain its temperature at the level needed to sustain thermionic electron emission.

5. Ions recombine at the wall surfaces they reach and re-enter the cathode interior plasma as neutral atoms. Neutral atoms must leave the cathode interior through the orifice at their supply rate.

6. As electrons pass through the orifice they are accelerated through a several volt potential difference which gives them sufficient energy so they can ionize some of the neutral atoms that are escaping through the orifice with them.

7. The ions and electrons downstream of the orifice constitute the plasma plume that is essential to the plasma contacting process. These species are lost by either going to nearby surfaces (e.g. the anode or cathode) where they recombine or through the interface between the contactor plume and the near-field ambient plasma shown in Fig. 1.

Apparatus and Procedures

In order to study the plasma contacting process experimentally, the apparatus shown schematically in Figs. 3 and 4 was constructed. Physically this apparatus consists of two hollow cathode devices, one (shown at the right of each figure and labeled "simulator") used to generate a simulated ambient plasma and the other (shown at the left and labeled "contactor") used to generate a contactor plasma plume that is biased relative to the ambient plasma to induce current flow. Also shown are the power supplies and instrumentation needed to sustain and measure the characteristics of the plasmas produced. The simulator and contactor hollow cathodes are separated by 2.7 m and are located within a 1.2 m dia. by 5.3 m long vacuum chamber. They both utilize cathodes with 6.4 mm dia. orifice plates and inserts that were fabricated by rolling 0.013 mm thick tantalum foils into the shape of a hollow cylinder and treating them with chemical R-500*.

The orifice in the simulator cathode is 0.38 mm in diameter and its anode is a solid 3.0 cm dia., 0.25 mm thick tantalum plate oriented parallel to the orifice plate and separated from it by a distance that could be varied from 1 to 5 mm. The orifice in the contactor cathode is, on the other hand, 0.76 mm in dia. Its anode is a 12 cm dia. stainless steel plate with a 1 cm dia. tantalum insert having a 5 mm dia. orifice in it. The anode plate, insert and orifice are all located concentric with the cathode centerline on a plane -2 mm downstream of the cathode orifice plate.

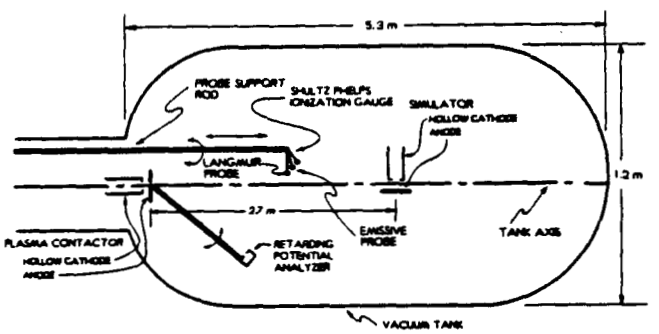

Fig. 3. Mechanical Schematic Diagram

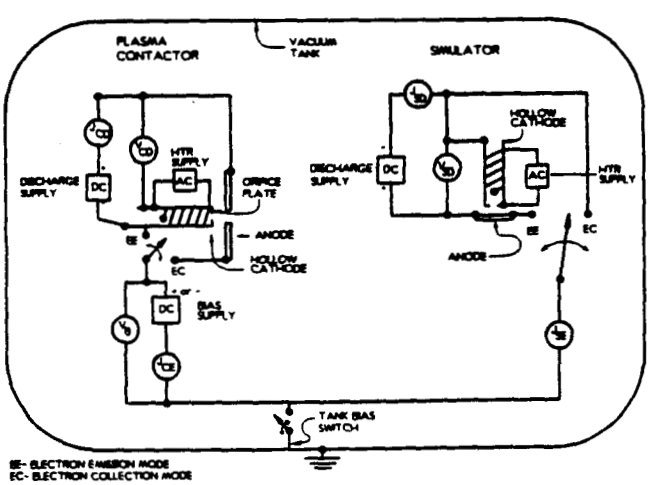

Fig. 4. Electrical System Schematic

Typical tests were conducted by heating the contactor and simulator cathodes to temperatures where significant thermionic electron emission could occur (~1300 K), establishing high expellant (xenon) flowrates through them, and biasing their anodes positive using the discharge supplies to initiate cathode-to-anode discharges at each device. Next, the desired contactor and simulator flowrates ($\dot{m}_c$ and $\dot{m}_s$) and discharge current levels (J_{CD} and J_{SD}) were established; the contactor was biased relative to the simulator using the bias power supply; and voltage, current and probing instrument data were collected. The voltages and currents measured during typical tests are designated by the symbols shown within the circles in Fig. 4; they include the contactor and simulator discharge currents and voltages (J_{CD}, J_{SD}, V_{CD} and V_{SD}), the bias voltage between the contactor and simulator (V_B) and the contactor and simulator electron emission currents (J_{CE} and J_{SE}).

The two switches shown at the contactor and simulator in Fig. 4 are positioned at either the "EE" or "EC" position depending on whether the contactor is biased negative of the simulator and therefore Emitting Electrons (EE) or biased positive and therefore Collecting Electrons (EC). It is necessary to position these switches properly for each operating mode to assure that intentional limitations imposed on the discharge current levels (J_{CD} and J_{SD}) do not result in unintentional limitations being imposed on the electron emission or collection currents.[7]

The tank bias switch shown in Fig. 4 was installed so the vacuum tank could be allowed to float relative to the contactor/simulator system or be connected to the simulator. Tests conducted to investigate the effects of changes in the position of this switch on plasma and performance data have suggested that it has no significant effect on a contactor collecting electrons. On the other hand, when the contactor is emitting electrons and the switch is closed, most of the electron current is drawn to the tank while most of this electron emission current must flow to the simulator when the tank is floating. Emitting electrons with the switch open was therefore found to induce higher bias voltages and current flow and plasma density patterns that tended to be concentrated along the tank centerline rather than being distributed uniformly in the tank. This occurred because all of the emitted electrons were being forced into collection at the simulator and this distorted the current flow patterns away from the spherical symmetry that would be expected in space. In order to conduct tests that were considered to be more representative of those expected in space, tests described herein were generally conducted with the tank bias switch closed. Any data collected with this switch open, will be identified specifically.

The plasma environment produced between the contactor and the simulator was probed using the various instruments shown in Fig. 3. These instruments, the function they serve and the physical volume in which they can be used are:

Emissive Probe - This sensor and the associated circuitry system, which are similar to

*Chemical R-500 is a double carbonate ($BaCO_3$, $SrCO_3$) low work function mixture that has been made by J.T. Baker Co. but is no longer in production.

those used by Aston,[8] yield plasma potential data directly. The sensor can be swept axially downstream from the contactor to the simulator and/or radially along an arc that extends from the tank/contactor centerline out to a radius of -30 cm. Probe output voltage (i.e. plasma potential) and position are recorded simultaneously on an X-Y plotter to assure well-correlated values of the data.

Langmuir Probe - The sensor used on this probe is a 3.2 mm dia stainless steel sphere that can be moved conveniently into any position occupied by the emissive probe. Probe current/voltage characteristic curves recorded at these positions are analyzed using a two electron-group numerical model[9] that is assumed to describe plasmas such as these. This analysis yields the density and temperature of a Maxwellian electron group and the density and energy of a primary (or monoenergetic) electron group. This analysis is aided by inputting plasma potential data determined using the emissive probe at each location where Langmuir probe data are collected. The circuitry together with additional detail about the numerical procedures used to obtain plasma information have been described previously.[10]

Shultz-Phelps Ionization Gauge - This commercially available pressure gauge[11] was modified by removing the glass enclosure around the sensor so perturbations to static pressure measurements that could have been induced by gas flows through the cathode, would be minimized and so its spatial resolution would be improved. This probe was used to measure the ambient pressure distributions over the same region swept by the emissive and Langmuir probes. Neutral atom density distributions were computed from these data by applying the perfect gas state equation and assuming the ambient gas was in equilibrium with the vacuum tank walls at a temperature of 300 K. Because gauge readouts from this device are inaccurate when a plasma is present, the measurements were made only when the cathodes were at operating temperatures and flowrates and the plasma discharges were extinguished.

Retarding Potential Analyzer - The sensor on this instrument was designed so it could be swept through an arc that passed through the tank centerline, was centered at the cathode orifice, and had a radius of about 18 cm. In the course of moving through this arc its aperture remained pointed at the cathode orifice. It was biased so it repelled both electrons and low energy ions and therefore sensed the current density of high energy ions that approached it from the location of the cathode.

Results

When a typical hollow cathode plasma contactor is biased relative to an ambient plasma and the voltage difference between it and the ambient plasma in contact with it is measured as a function of the electron current being emitted, data like those shown in Fig. 5 are obtained. These particular data were obtained at a contactor discharge current (J_{CD}) of 0.3 A and an expellant flowrate ($\dot{m}_c$) of 4.1 standard cubic centimeters per second (sccm) of xenon. Under these conditions the ambient neutral gas pressure (P_o) in the vacuum tank was 5×10^{-6} Torr and the contactor discharge voltage (V_{CD}) varied over the range from 12 to 20 V as the electron emission current (J_{CE}) was varied from +1000 mA to -1000 mA. The contactor potential plotted on the horizontal axis in this figure is actually the difference between the contactor anode or cathode potential (V_B) and the ambient plasma potential (V_p) sensed by an emissive probe located ~1 m downstream of the contactor. The data of Fig. 5 show the contactor potential remains near -25 V when the contactor is emitting electrons (second quadrant) and that the contactor rises to about 50 V when the contactor is collecting electrons (i.e. for negative emission currents in the fourth quadrant).

The curve in the fourth quadrant of Fig. 5 shows that the magnitude of the electron collection current increases rather suddenly at a potential difference of -40 V where the "transition to ignited mode" operation is identified. This transition has generally been observed to occur as contactor potential is being increased. Its onset is accompanied by the appearance of a bright luminous glow that typically extends several centimeters from the contactor and is somewhat spherical in shape. It is believed that this luminosity is caused by the de-excitation of xenon atoms that have been excited by electrons being drawn (streaming) toward the contactor. It is presumed that some ionization is also induced along with these excitation reactions.

Electron Collection

When plasma potentials are measured throughout the region immediately downstream of a contactor collecting electrons, data like those shown in Fig. 6 are obtained. This figure includes both a raised potential map, which clearly shows the

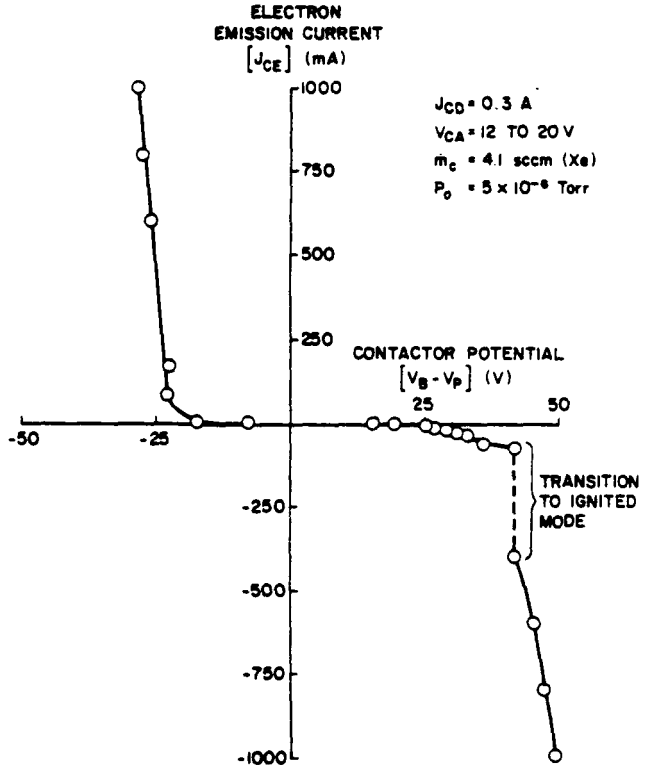

Fig. 5. Typical Plasma Contactor Performance Curve

structure of the plasma field around the contactor qualitatively and an equipotential contour map from which quantitative information about the potentials can be obtained. These two plots show the plasma field consists of two relatively uniform potential plasma regions separated by a region in which the potential gradients are large. Since neither magnetic field nor collisionally induced impedances are present in the region where the potential changes rapidly, this must be a sheath region,[12] i.e. one in which charged particle acceleration is occurring.

On the basis of the typical data of Fig. 6 one can propose the model of the near-field electron collection process suggested by Fig. 7. This model involves a relatively higher density plume of quasi-neutral plasma in the region immediately adjacent to the contactor separated from a lower density quasi-neutral ambient plasma by a double-sheath (or double-layer). As the centerline plasma potential profile in this figure suggests, electrons and ions counterflow through the double-sheath. Specifically, electrons from the ambient plasma are drawn toward the contactor plasma plume and ions from this plume are drawn toward the ambient plasma. On the other hand, ions from the ambient plasma and electrons from the contactor plume are both reflected at the sheath. The ion and electron currents that can be drawn through the double-sheath region are limited by the space-charge effects suggested by the net accumulations of positive and negative charge shown, respectively, upstream and downstream of the sheath midpoint in the bottom sketch of Fig. 7.

When plasma properties are measured along the vacuum tank/contactor centerline through a typical double-sheath, data like those shown in Fig. 8 are obtained. These results suggest plasma conditions do vary in a way that is consistent with the model of Fig. 7 (note that the zero voltage for the plots of Figs. 6 and 7 is the ambient plasma potential, while that for Fig. 8a is the simulator cathode potential). Figures 8b and c indicate the high density and ambient plasmas are both composed of primary (monoenergetic) and Maxwellian electron groups. They show the Maxwellian temperature and density and the primary energy and density all remain constant at about 6 eV, 4 x 10^7 cm^{-3}, 40 eV and 3 x 10^6 cm^{-3} respectively, in the ambient plasma region for this case where ~370 mA of

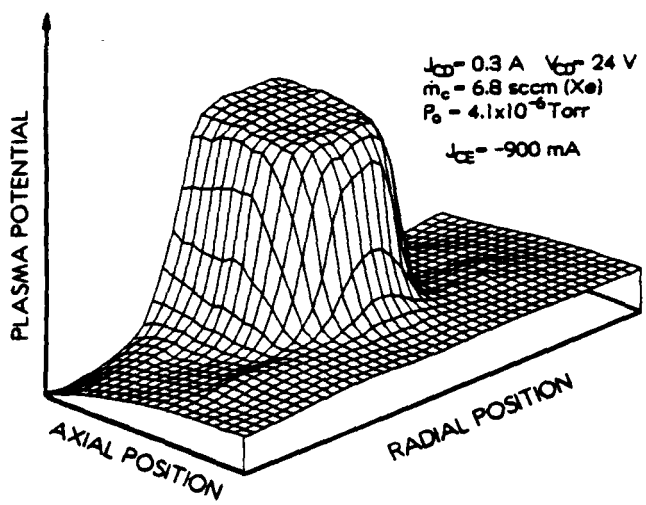

a. Raised Potential Map

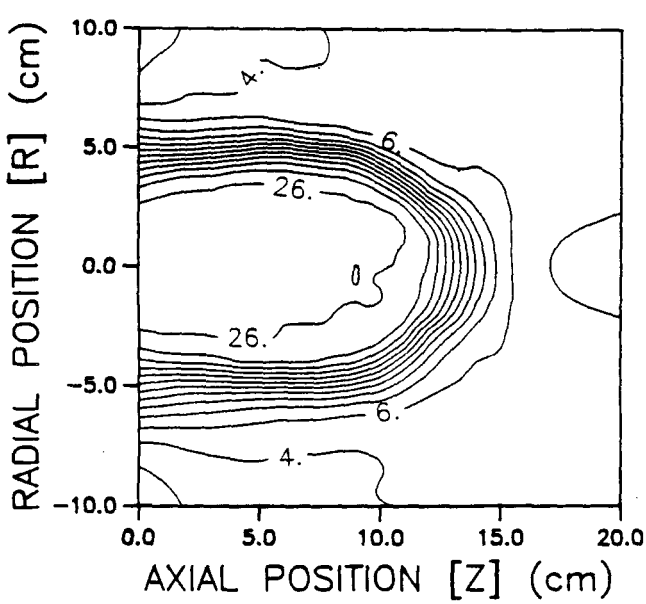

b. Equipotential Contour Map

Fig. 6. Typical Potential Variation near a Contactor Collecting Electrons

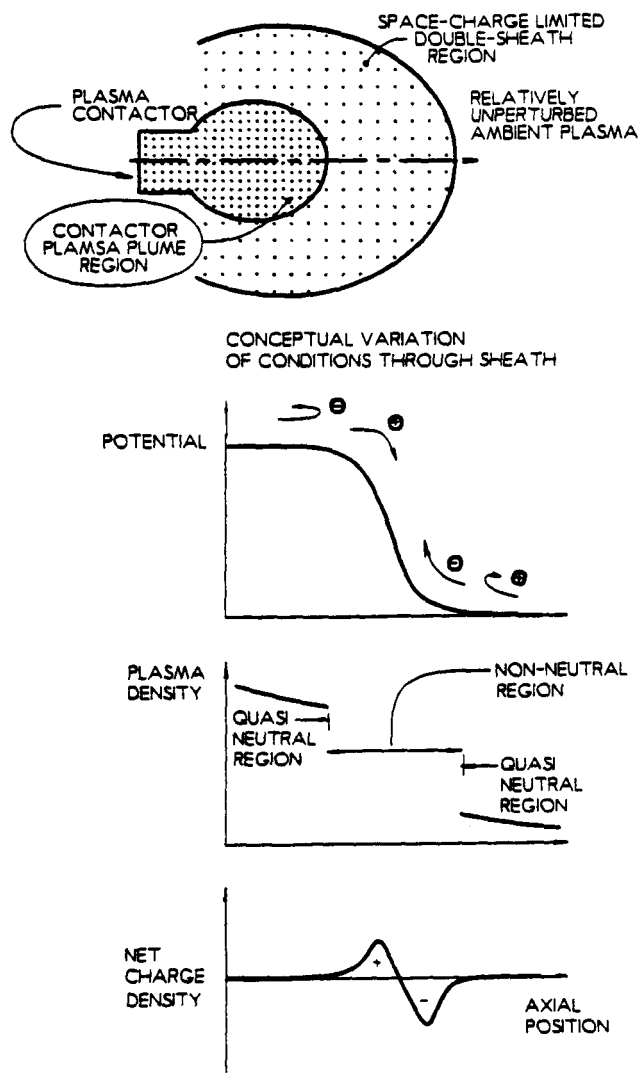

Fig. 7. Conceptual Model of the Near-Field Electron Collection Process

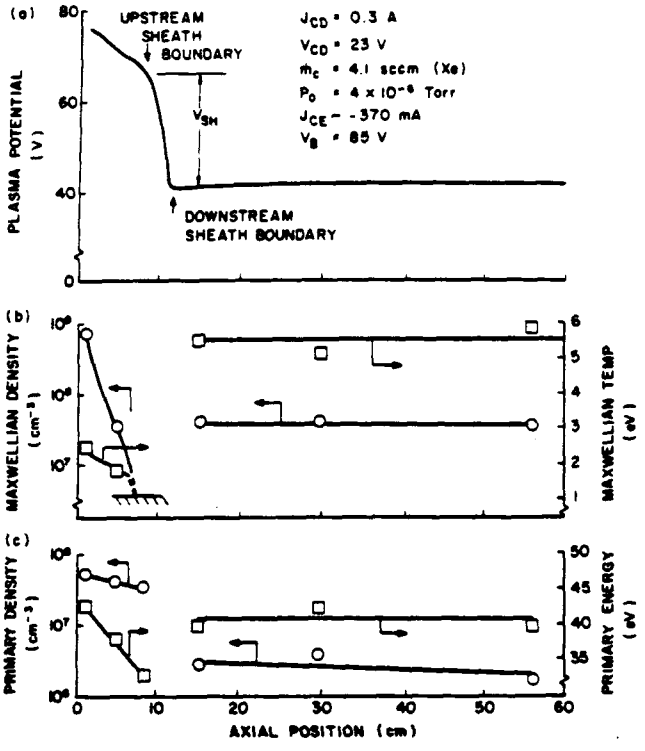

Fig. 8. Typical Plasma Property Profiles Measured along the Centerline - Electron Collection Mode

electrons are being collected.

It is noted that the energy of the primary electrons in the ambient plasma (Fig. 8c) is approximately equal to the simulator cathode-to-ambient plasma potential difference. This suggests that these electrons are ones that have been accelerated into the ambient plasma from the simulator hollow cathode and have had few energy-degrading collisions. It should be noted that the ratio of primary-to-Maxwellian electrons in the ambient plasma is small (usually less than 10% as in the case of the data of Fig. 8). The data of Fig. 8b show the density of the Maxwellian electrons upstream of the double-sheath drops rapidly with distance from the contactor cathode. The floor symbol drawn on Fig. 8b near the double-sheath location indicates that the Maxwellian density and temperature were not measurable at this location because the primary electron signal to the Langmuir probe overwhelmed the Maxwellian one. The data of Fig. 8c show the primary electron density upstream of the sheath is more than an order of magnitude greater than that downstream. The primary electron density upstream of the sheath is also seen to increase as the distance from the contactor decreases probably because these electrons are being concentrated as they stream radially inward toward the cathode. Finally, it should be noted that the energy of the primary electrons in the region upstream of the sheath (35 to 45 V) is roughly equal to the sheath potential drop (V_{SH}). This suggests that the primary electrons found in the high density plume are indeed those that have been accelerated across the sheath from the Maxwellian electron group in the ambient plasma. This result also supports the proposed physical model of the electron collection process.

Theoretical Model of Electron Collection

Conversion of the basic physical model of near-field electron collection into a quantitative model requires that the unknowns of the problem (sheath location and voltage drop for example) be expressed mathematically in terms of such known or controllable parameters and variables as the current being collected and the ambient and contactor plume plasma densities and temperatures. An elementary theoretical model of the electron collection process has been developed and verified using experimental results obtained in the laboratory.[13] The essential features of this model reflect the observations that 1) the surface area of the downstream boundary of the double-sheath is determined by the electron current being collected and the random electron current density in the ambient plasma, 2) the surface area of the upstream boundary of the double-sheath is determined by the space-charge-limited ion current that must flow across the sheath at a current density defined by the Bohm condition for a stable sheath[14] and 3) the voltage drop across the sheath is determined by the requirement that ions and electrons flow across the sheath at their space-charge-limited levels.[15]

If it is assumed that electron collection is spherically symmetric and that it occurs over a full 4π steradian solid angle, then the first condition identified in the previous paragraph requires that the outer radius of the double-sheath (r_o) be given by

$$r_o = \left[\frac{|J_{CE}|}{e\, n_o}\sqrt{\frac{m_e}{8\pi\, k\, T_{eo}}}\right]^{1/2} \qquad (1)$$

where $|J_{CE}|$ is the magnitude of the electron collection current, e is the electron charge, n_o and T_{eo} are the ambient plasma density and electron temperature, k is Boltzmann's constant and m_e is the electron mass.

Imposition of the second condition for the same case leads to the following expression for the inner radius of the double-sheath

$$r_i = \left[\frac{J_+}{4\pi\, e\, n_i\, \gamma}\sqrt{\frac{m_+}{k\, T_{ei}}}\right]^{1/2} . \qquad (2)$$

In Eq. 2, J_+ is the ion current being supplied to the sheath from the contactor plume, n_i and T_{ei} are the plasma density and electron temperature in the contactor plume, γ is a pre-sheath correction parameter that is projected to have a value of 0.3 based the laboratory tests,[13] and m_+ is the mass of the ions being supplied from the plume.

Imposition of the third condition yields the voltage drop (V_{SH}) that develops across the double-sheath

$$V_{SH} = \left[\frac{|J_{CE}|}{4\pi\, \epsilon_o\, j_o}\left(\frac{m_e}{2e}\right)^{1/2}\right]^{2/3} . \qquad (3)$$

In this equation ϵ_o is the permittivity of free space and j_o is a parameter determined by the solution to the spherical space-charge-limited,

double-sheath problem.[15] The variation of this parameter as a function of double-sheath radius ratio is reproduced from Ref. 15 in Fig. 9.

The Effects of Ion Current on Electron Emission Behavior

In order for the model expressed in the preceeding equations to be valid, the contactor plume should be spherical and the ion and electron currents should both be flowing at their space-charge limited values. This means that the ion current flowing from the contactor plume to the ambient plasma (J_+) must given by

$$J_+ = \frac{|J_{CE}|}{\alpha}\sqrt{\frac{m_e}{m_+}} \quad , \qquad (4)$$

where α is a parameter determined from the solution of the space-charge current flow problem.[15] The variation in this parameter with double-sheath radius ratio is reproduced from Ref. 15 in Fig. 10.

Figure 11 shows the effect of changes in the ion current density flowing across a typical double-sheath, as a function of the electron current being collected through that sheath. These measurements were made with the retarding potential analyzer positioned on the tank centerline under conditions where the double-sheath radius ratio did not change significantly as collection current was varied. This figure demonstrates that the measured

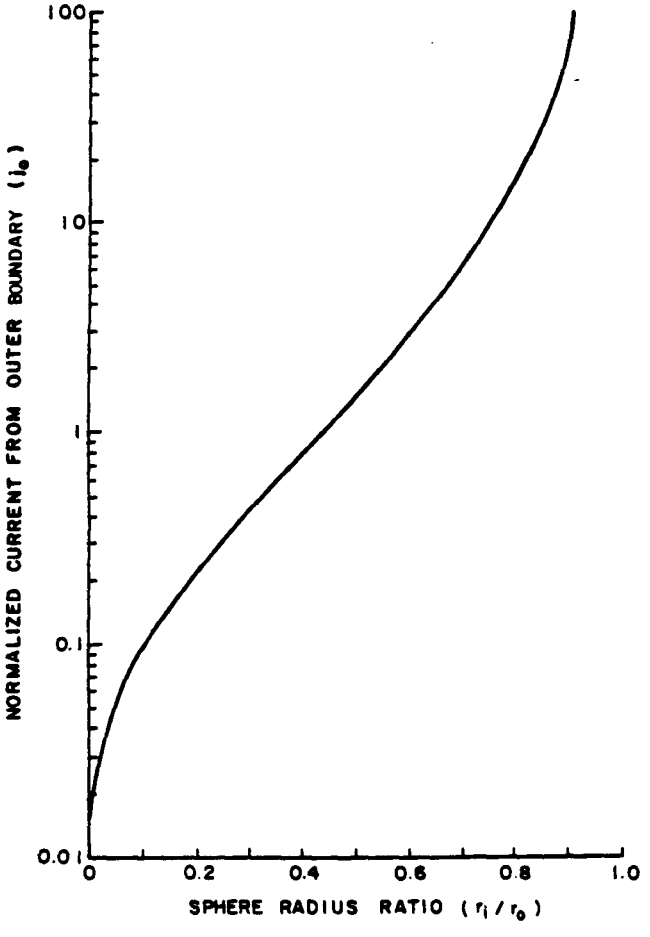

Fig. 9. Effect of Radius Ratio on Space-Charge-Limited Current Magnitude

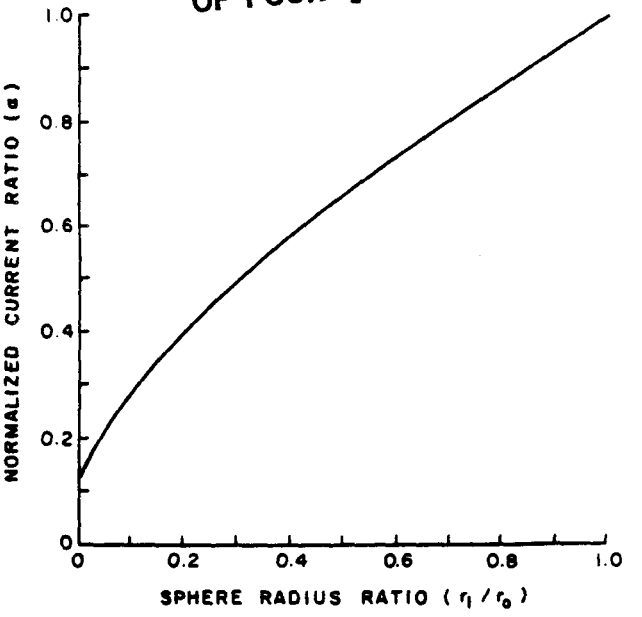

Fig. 10. Effect of Radius Ratio on Counterflowing Current Ratio

functional relationship between the ion and electron currents (linear) is in excellent agreement with Eq. 4. Measurement of the azimuthal variation in the ion current density through a typical sheath using the retarding potential analyzer and integration of the resulting profile yields a total ion collection current that agrees quantitatively with the prediction of Eq. 4 to within a factor of two. These results are considered to be a verification that ion and electron current flows through typical double-sheath are space-charge-limited.

Ignited Mode Electron Collection

The rather sudden increase in electron collection current shown in the data of Fig. 6 that is accompanied by the development of luminosity in the high density plume region is an important phenomenon. When this transition into the ignited mode of electron collection occurs, the slope of the current/voltage characteristic becomes more negative and lower sheath voltage drops are required at a given electron collection current. It is believed that this occurs because electrons

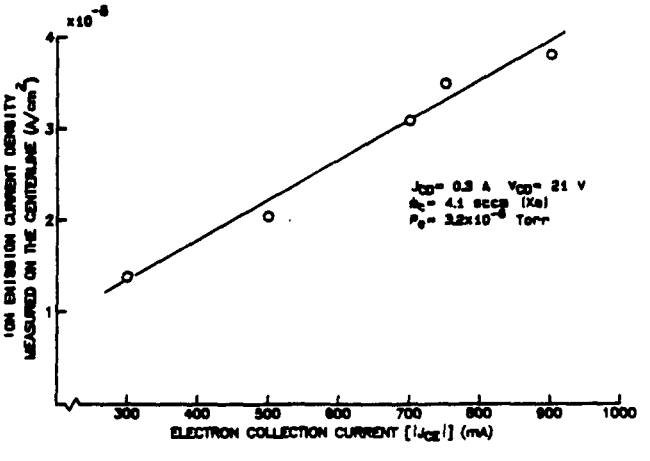

Fig. 11. Effect of Electron Collection Current on Ion Emission Current Density

being collected, acquire sufficient energy on passing through the sheath so they can excite and ionize expellant atoms coming through the cathode orifice. The excitation would be expected to cause the observed increase in contactor plume luminosity, and the ionization would be expected to cause an increase in the ion current leaving the plume. This would in turn be expected to cause the observed increase in electron collection current (c.f. Eq. 4).

In order to assure that sufficient excitation and ionization reactions do occur to induce "ignited mode" operation, it is necessary to determine if the neutral atom density is sufficient to give a reasonable electron-atom inelastic collision frequency. The raised density and equal density contour plots of Fig. 12 show the axial and radial variation in xenon atom density measured immediately downstream of the contactor at typical contactor ($\dot{m}_c$) and simulator ($\dot{m}_s$) flow conditions which induce the indicated ambient pressure (P_o). These data have been computed on the basis of pressure measurements by applying the perfect gas equation and assuming the gas is in equilibrium with the vacuum chamber wall at a temperature of

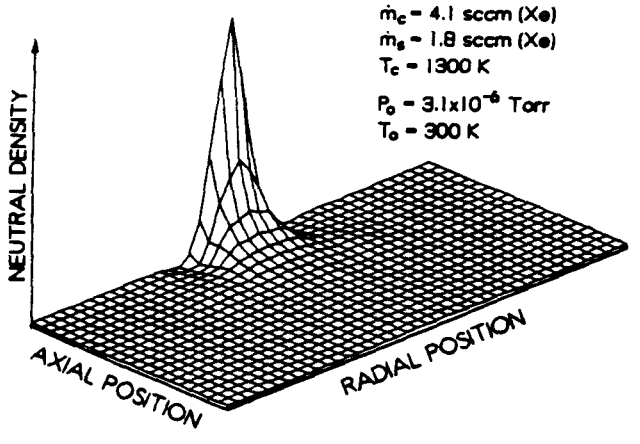

a. Raised Neutral Density Map

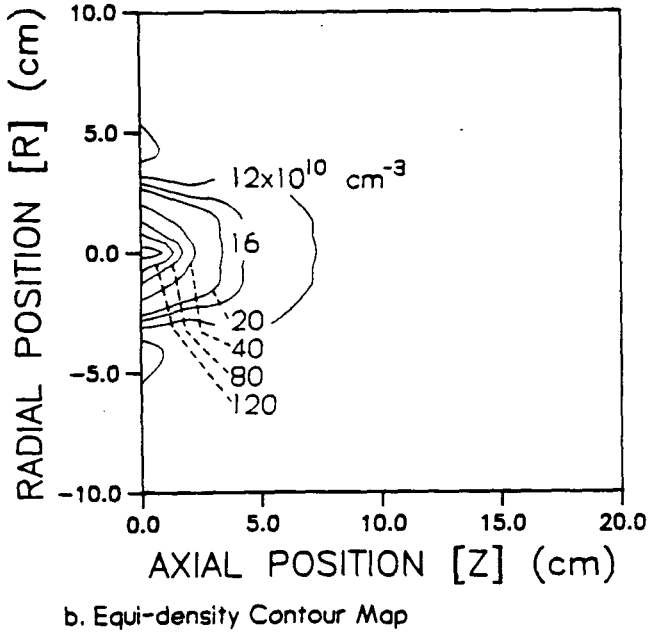

b. Equi-density Contour Map

Fig. 12. Typical Variation in Neutral Atom Density

300 K. They suggest the density drops from a high value at the contactor orifice to background levels at distances several centimeters from it.

Using data like those shown in Fig. 12, typical ion production rates due to electrons streaming toward the contactor cathode can be computed.[16] Typical results obtained from such calculations are shown in Fig. 13 in the form of a plot of integrated ion production rate by electrons that have streamed from the inner radius of the sheath to the radius values indicated on the horizontal axis. The calculations have been made for two cases using experimentally measured sheath voltage drops (V_{SH}), sheath radii, etc. The curves indicate that the ion production rate increases dramatically as the streaming electrons approach the contactor orifice ($r \rightarrow 0$) because the xenon density is highest there. The location of the arrows on each curve (at ~ 1 cm) indicate the radial positions where the ion production due to streaming electrons alone would be sufficient to satisfy the space-charge-limited ion current criterion at the electron current being collected (J_{CE} = -1.0 A). Hence it is suggested that ion production induced by streaming electrons alone could be sufficient to assure low voltage operation of a contactor collecting electrons without including any ions produced in the hollow cathode-to-anode discharge. It is noted in this regard that discharge produced ions are generated sufficiently close to the cathode so they can recombine on hollow cathode or anode surfaces more readily than ions produced by streaming electrons. It is considered likely that essentially all ions produced within a few Debye shielding lengths of the cathode (identified in Fig. 13) by either mechanism would be lost to the cathode.

It is considered to be particularly noteworthy that the discharge current (J_{CD}) a contactor may be reduced to zero without inducing a change in the sheath voltage drop once the contactor is collecting electrons stably in the ignited mode. This observation also supports the hypothesis of substantial ion production by streaming electrons.

Electron Emission Mode of Operation

Each contactor used on an electrodynamic tether will probably be designed as both an electron emitter and an electron collector. Since hollow cathode contactor operation has been demonstrated in space in the electron emission mode at relatively high current levels[17,18] this mode

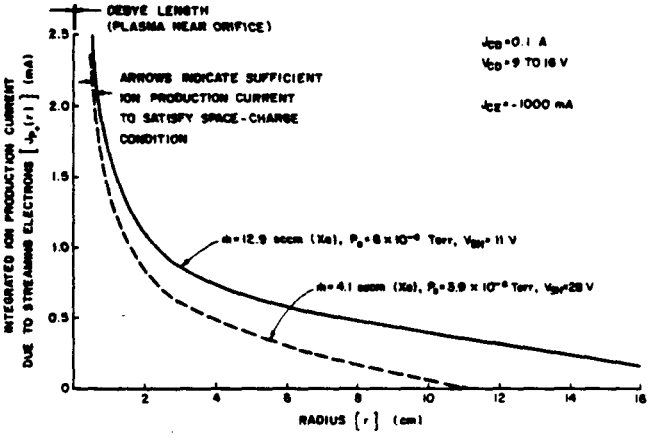

Fig. 13. Effect of Flowrate on Ion Production by Streaming Electrons.

ORIGINAL PAGE IS
OF POOR QUALITY

has been considered less problematic. As a result the early efforts at plasma probing and modeling the plasma contacting processes have focused on the less well understood electron collection mode of contacting. Data showing typical sheath voltage drops have been measured in the laboratory, however, and these results (like those in Fig. 5) suggest that the sheath voltage drops are lower for the electron emission mode than for the electron collection mode.

Figure 14 shows typical plasma potential maps measured for a contactor emitting electrons at a current level of 1.25 A. These maps differ from those for a contactor collecting electrons because they show no uniform plasma potential region adjacent to the contactor. Because such a region is not apparent it has not been possible to apply the simple double-sheath model to this case even though electrons and ions would be expected to counterflow at their space-charge-limited levels in the electron emission mode just as they appear to in the electron collection mode.

As the electron emission current level is reduced, the associated potential profiles begin to show increased structure like that in Fig. 15, where potentials that rise from zero in the ambient plasma to about 3 V before they drop below -5 V in the plasma adjacent to the contactor orifice. In this lower current case the potential hump (at ~3 V) suggests a net positive space-charge accumulation develops, presumably because electrons streaming from the cathode with substantial kinetic energies ionize neutral atoms and leave behind slow-moving ions.[12] The reason why a potential hump should develop at emission current levels (Fig. 15) and not high ones (Fig. 14) is not apparent, however, if this is the mechanism by which the hump is produced. A careful analysis of the data has suggested the hump probably develops to an even greater extent at the higher current levels, but the emissive probe does not measure it properly. This measurement error can be understood by recognizing that an emissive probe; which is being held at a relatively high, but constant, temperature so it will emit electrons; measures a floating potential that is close to the true plasma

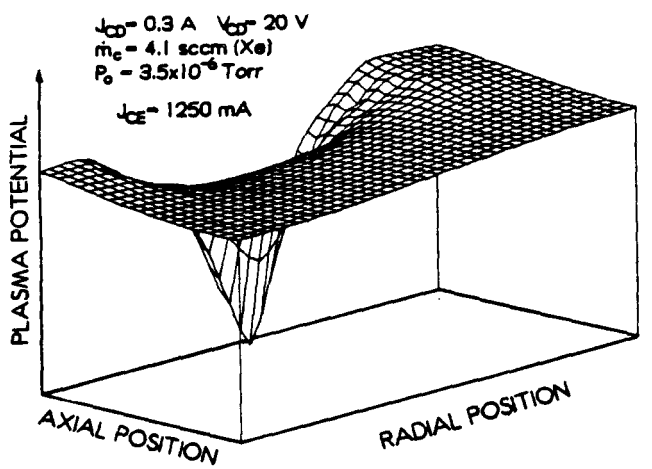

a. Raised Potential Map

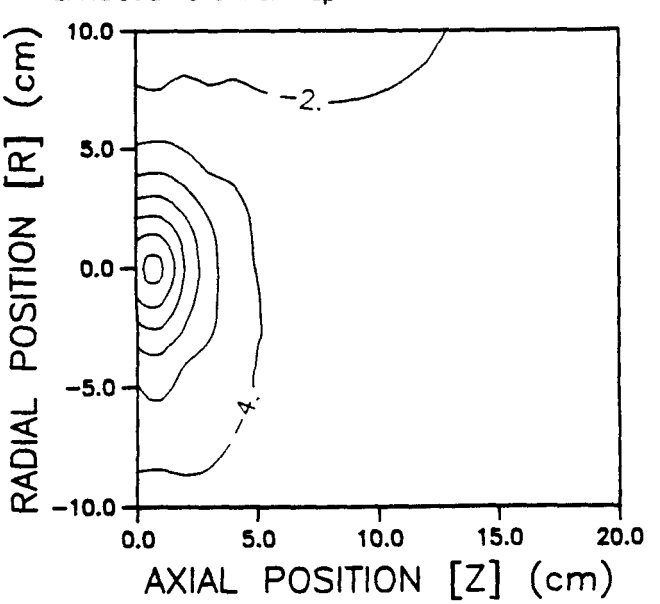

b. Equipotential Contour Map

Fig. 14. Typical Potential Variation near a Contactor Emitting Electrons at a High Current Level

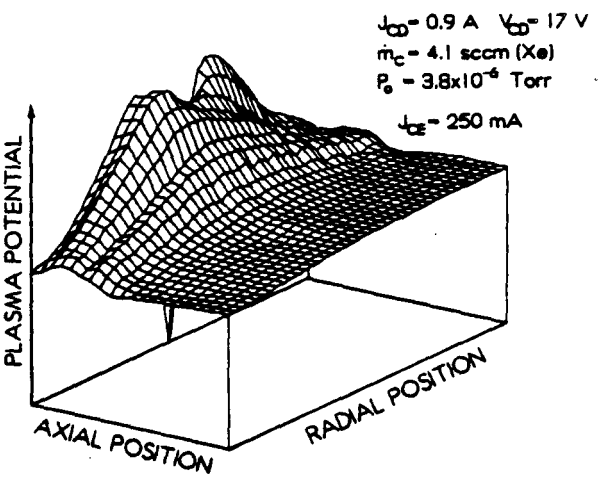

a. Raised Potential Map

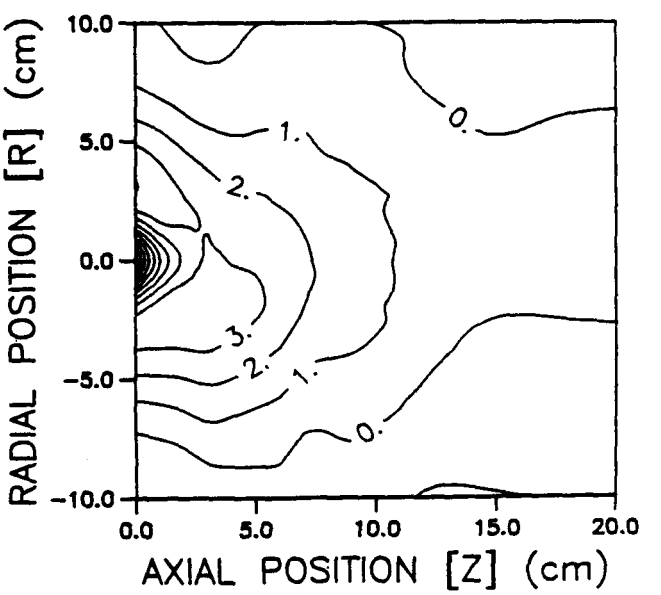

b. Equipotential Contour Map

Fig. 15. Typical Potential Variation near a Contactor Emitting Electrons at a Low Current Level

potential when it is in a low density plasma. As it is moved into more dense plasmas however, it floats at potentials that drop progressively further below the true potential of the plasma. This occurs because the thermal current of electrons from progressively more dense plasma eventually exceeds the thermionic emission capability of the probe.

It is noted that the data of Fig. 15 were collected under an operating condition that was essentially the same as that for the case where the tank switch (Fig. 4) was open because this produced a more dramatic potential hump. Detailed studies of the electron emission mode of operation are presently being conducted to determine why this occurs and to develop an understanding of the electron emission process that will lead to a model that can be used to describe it physically and mathematically.

Extending Laboratory Results to Space

It should be recognized that an ideal experimental simulation of the in-space plasma contacting process would involve similarity of not only the current levels and contactor hardware involved, but also the space environment. Complete simulation of this environment implies 1) similar ambient ionic/atomic species concentrations, 2) similar ambient plasma density and temperature levels, 3) similar magnetic field intensity and relative contactor/magnetic field velocity conditions, and 4) an ambient plasma that is not perturbed by vacuum chamber walls or other apparatus during the conduct of the tests. In the present study these conditions have in general not been met.

Specifically, no attempt has been made to simulate the ionic and atomic species of space; rather the background gas in the tests is principally xenon coming from the contactor and simulator. Further, it has been found that electrons being emitted or collected by the contactor and simulator collide with the background gas and produce ions at a rate that has a far greater influence on the ambient plasma density and temperature than does the simulator discharge current and voltage. As a result, ambient plasma densities used in the tests are substantially greater than those expected during the conduct of space tests. This high plasma density has the beneficial effect, however, of preventing the contactor plasma plume/double-sheath from extending to and interacting with the vacuum chamber walls. If the tests had been conducted at the low densities of space an unreasonably large vacuum chamber would have been required to prevent such an interaction from occurring.

While some effects of changes in magnetic field strength on the plasma contacting process have been examined[7] and been found to have a negligible influence on laboratory test results, the effects of magnetic field strength and relative motion at space plasma density conditions are not reflected in any test results. It is suggested, however, that the skin depth associated with a typical ionospheric plasma propagating at low earth orbital velocity will be small compared to contactor plasma plume dimensions realized during the conduct of typical space tests. Hence it is argued that one may separate near and far-field effects in the manner suggested in Fig. 1 and that the tests conducted do reflect the basic physics of the important near-field phenomena.

It is suggested on the basis of the review of the differences between the laboratory and space plasma experiments just discussed that results obtained from space tests may differ substantially from those measured in laboratory tests. The laboratory results can, however, be used to identify phenomena that will probably be important in space, and they can serve to calibrate numerical models of the contacting process[19] that do reflect the effects of magnetic fields, spacecraft motion, and accurate ionospheric properties.

Conclusions

Plasma contacting represents an effective means of preventing various types of spacecraft charging problems and it is therefore an enabling technology in the many applications where this phenomenon is likely to occur.

The near-field plasma contacting process associated with electron collection can be described using three distinct regions in which different plasma properties and particle acceleration phenomena prevail. These are a contactor plasma plume region that is immediately adjacent to the contactor, a double-sheath region and a near-field ambient plasma region. Beyond these regions it is presumed the effects of motion of the near-field plasma relative to the ionospheric plasma and the magnetic field within it become important.

Ions and electrons counterflow through the collisionless double-sheath to conduct current between contactor and near-field ambient plasmas biased relative to each other. The outer boundary of this double-sheath is located such that its surface area is sufficient to collect the electron current being drawn from an ambient plasma characterized by a prescribed random electron current density. The inner boundary of the double-sheath is located such that its surface area is sufficient to supply an ion current at a rate that will satisfy both the Bohm criterion on sheath stability and the space-charge limit on ion extraction. The bulk of the voltage drop associated with the near-field electron collection process develops between these two boundaries of the double-sheath. This voltage difference establishes itself at a value that will assure both the ion and electron currents flow at their space-charge-limited values.

Electron collection is most efficient when the contactor is operating in the "ignited mode". In this operating mode, electrons streaming from the ambient plasma excite and ionize expellant gas coming from the hollow cathode. Once operation in this mode develops it is possible to sustain the electron collection process without supplying power from the hollow cathode discharge supply.

References

1. Purvis, C.K., and R.O. Bartlett, "Active Control of Spacecraft Charging," Progress in Astron. Aeron., H.B. Garrett and C.P. Pike, eds., V. 71, 1980, p. 299-317.

2. Olsen, R.C., C.E. McIlwain and E.C. Whipple, "Observations of Differential Charging Effects on ATS 6," J. Geophys. Res., V. 89, No. A8, 1981, pp. 6809-6819.

3. Sisson, J.M., "Development Status of First Tethered Satellite System," AIAA Paper 86-0049, Jan. 6-9, 1986, Reno, Nevada.

4. Wilbur, P.J., "Hollow Cathode Plasma Coupling Study-1986," NASA CR-171985, Dec. 1986.

5. Burch, J.L., Southwest Research Institute letters to Dr. Dixon M. Butler, Dr. Robert D. Hudson, Dr. David L. Reasoner, Dr. S.D. Shawhan, Dr. N.H. Stone and Dr. M. Torr, conveying Charge Neutralization Workshop Resolution, Sept. 9, 1985.

6. Siegfried, D.E. and P.J. Wilbur, "A Model for Mercury Orificed Hollow Cathodes: Theory and Experiment," AIAA Journal, V. 22, 1984, pp. 1405-1412.

7. Williams, J.D., "Electrodynamic Tether Plasma Contactor Research," appears in Advanced Electric Propulsion and Space Plasma Contactor Research, NASA CR-180862, P.J. Wilbur, ed., Jan. 1987, pp. 1-75.

8. Aston, G. and P.J. Wilbur, "Ion Extraction from a Plasma," J. Appl. Phys., V. 52, No. 4, April 1981, pp. 2614-2626.

9. Beattie, J.R., "Numerical Procedure for Analyzing Langmuir Probe Data," AIAA Journal, V. 13, No. 7, July 1975, pp. 950-952.

10. Laupa, T. "Thick Sheath Langmuir Probe Trace Analysis," appears in Advanced Electric Propulsion and Space Plasma Contactor Research, P. Wilbur, ed., NASA CR-175119, Jan. 1986, pp. 128-138.

11. Anon., "Instruction Manual No. 0-01-224017 for Ionization Gauge Controllers,' Granville-Phillips Co., Boulder, CO, 1971.

12. Langmuir, I., "The Interaction of Electron and Positive Ion Space Charges in Cathode Sheaths," Phys. Rev., V. 33, No. 6, June 1929, p.954-989.

13. Williams, J.D., P.J. Wilbur and J.M. Monheiser, "Experimental Validation of a Phenomenological Model of the Plasma Contacting Process," appears in Space Tethers for Science in the Space Station Era, L. Guerriero and I. Bekey, eds., Conference Proceedings, V. 14, Societa Italiana di Fisica, Venice, Oct. 4-8, 1987, pp. 241-244.

14. Bohm, D. "Minimum Ionic Kinetic Energy for a Stable Sheath," The Characteristics of Electrical Discharges in Magnetic Fields, A. Guthrie and R.K. Wakerling, eds., McGraw-Hill, New York, 1949, pp. 77-86.

15. Wei, R., and P.J. Wilbur, "Space-charge-limited Current Flow in a Spherical Double Sheath," J. Appl. Phys., V.60, Oct. 1, 1986, pp. 2280-2284.

16. Williams, J.D. "Electrodynamic Tether Plasma Contactor Research," appears in Space Plasma Contactor Research-1987, P.J. Wilbur, ed., NASA CR-182148, Jan 1988.

17. Kerslake, W.R. and L.R. Ignaczak, "SERT II 1980 Extended Flight Thruster Experiments," AIAA Paper 81-0665, Las Vegas, NV, 1981.

18. Kerslake, W.R., "SERT II Thrusters - Still Ticking after Eleven Years," AIAA Paper 81-1539, Colorado Springs, CO, 1981.

19. Katz, I. and V.A. Davis, "On the Need for Space Tests of Plasma Contactors as Electron Collectors," appears in Space Tethers for Science in the Space Station Era, L. Guerriero and I. Bekey, eds., Conference Proceedings, V. 14, Societa Italiana di Fisica, Venice, Oct. 4-8, 1987, pp. 241-244.

Appendix B

GROUND-BASED TESTS OF HOLLOW CATHODE PLASMA CONTACTORS

PRECEDING PAGE BLANK NOT FILMED

GROUND-BASED TESTS OF HOLLOW CATHODE PLASMA CONTACTORS*

John D. Williams† and Paul J. Wilbur**

Department of Mechanical Engineering
Colorado State University
Fort Collins, CO 80523

Abstract

Experimental results are presented which describe operation of and the plasma environment associated with a hollow cathode-based plasma contactor collecting electrons from an ambient, low density Maxwellian plasma when the boundary between the contactor and the ambient plasma is nearly hemispherical. Basic physical features of the process of electron collection identified on the basis of these results include a double-sheath across which a substantial potential difference can develop and substantial ionization of neutral gas coming from the cathode by the electrons being collected. Experimental results obtained when the diameter of the anode is too small to yield a hemispherical double-sheath are shown to induce distortion of this sheath but it is argued that the same basic phenomena are still active in this case. Data obtained in these experiments should serve to validate numerical models of this process that are being developed to predict plasma contactor performance in space. Preliminary performance and plasma property results measured on a contactor emitting electrons are examined and some physical elements of this process are identified.

Introduction

Hollow cathode-based plasma contactors have been shown to be effective in mitigating the undesirable charging of satellites.[1] The basic function of a plasma contactor is to create a highly conductive plasma in the region surrounding a satellite that can be used as a medium of current exchange to reduce voltage differences between the satellite and the local ionospheric plasma. Typically, the potential differences and current levels associated with this discharging process are small. When a plasma contactor is used in an electrodynamic tether application where relatively large currents must be exchanged with the ionosphere, however, potential differences would generally be expected to be greater. Because a large potential drop at a plasma contactor could seriously degrade the performance of an electrodynamic system,[2] it is important that one be able to understand, predict and control plasma contactor performance to prevent such voltage drops.

In general, two plasma contactors (one emitting electrons to the ionospheric plasma and one collecting them from it) are required to complete the circuit of a typical electrodynamic tether system. A hollow cathode discharge[3] has been proposed as a suitable plasma source for both of these contactor applications and these devices have been used to conduct the tests that are the basis of this paper. It is argued that the laboratory tests of hollow cathode contactors examined in these tests are similar to the near-field portion[3] of the plasma contacting process that will occur in space.

The operation of a contactor collecting electrons (i.e. one biased positive of a simulated space plasma so it will collect electrons) has received substantial experimental research attention.[3,4] This work has shown 1) a double-sheath develops between the contactor and ambient plasmas, 2) streaming electrons being collected ionize neutral atoms supplied through the cathode which can induce a more efficient mode of electron collection (ignited mode operation[3,4]) and 3) the double-sheath that develops in such tests can have a hemispherical shape and if it does, such characteristics as its position and the voltage drop across it can be described by a simple spherical double-sheath model[3,4]. This model describes phenomena occurring in three different regions, namely a high density, high conductivity plume adjacent to the contactor (the contactor plasma); a dilute plasma surrounding the contactor plasma which simulates the ionospheric plasma (the ambient plasma); and a relatively thin region between these two plasmas in which both the ion and electron flows are space-charge limited (the double-sheath region).

The intent of this paper will be 1) to present contactor performance and plasma property data associated with collection of electrons under conditions where a nearly hemispherical double-sheath develops, 2) to show that these results are consistent with the simple, spherical double-sheath model of the process, 3) to present similar data associated with operation under conditions where the double-sheath is distorted from the spherical shape and the simple model does not describe the measured behavior, 4) to argue, however, that the same physical phenomena are active when the double-sheath is distorted, and 5) to present preliminary data illustrating the basic physical phenomena associated with the electron emission process from a hollow cathode plasma contactor.

Apparatus and Procedure

In order to study the plasma contacting process experimentally, the apparatus shown schematically in Figs. 1 and 2 was constructed. The key elements of this apparatus are the two hollow cathode devices, one (shown at the right of each figure and labeled "simulator") used to generate a simulated ambient plasma and the other (shown at the left and labeled "contactor") used to generate a contactor plasma plume that is biased relative to the ambient plasma to induce current flow. Also shown in Figs. 1 and 2 are the power supplies and instrumentation needed to sustain and

*Work supported by NASA Lewis Research Center under Grant NAG 3-776.
†Research Assistant
**Professor, Member AIAA.

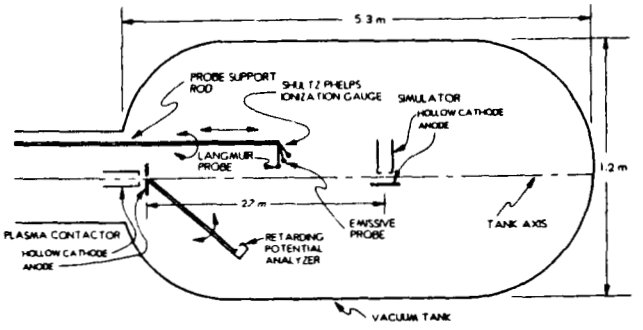

Fig. 1 Mechanical Schematic Diagram

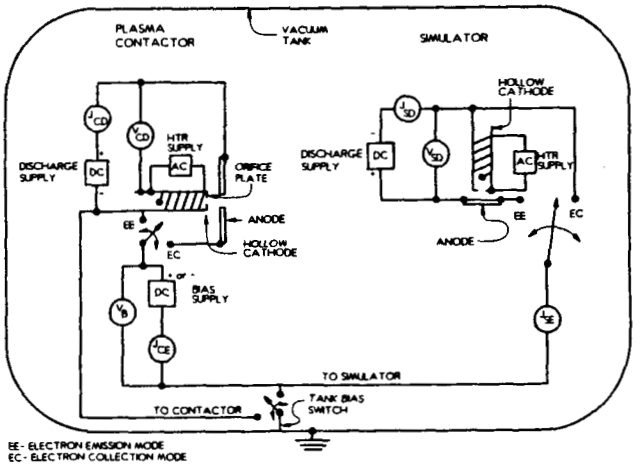

Fig. 2 Electrical System Schematic Diagram

measure the characteristics of the plasmas produced. The simulator and contactor hollow cathodes are separated by 2.7 m and are located within a 1.2 m diameter by 5.3 m long vacuum chamber. They both utilize cathodes with 6.4 mm diameter orifice plates and inserts that were fabricated by rolling 0.013 mm thick tantalum foils into the shape of a hollow cylinder and treating them with a low work function barium/strontium oxide material.

The orifice in the simulator cathode is 0.38 mm in diameter and its anode is a solid 3.0 cm diameter, 0.25 mm thick tantalum plate oriented parallel to the orifice plate and separated from it by a distance that could be varied from 1 to 10 mm. The orifice in the contactor cathode is, on the other hand, 0.76 mm in diameter. Its anode was either a 12 cm diameter, stainless steel plate with a 1 cm diameter tantalum insert having a 5 mm diameter orifice in it or a 3 cm diameter stainless steel plate with the same insert in it. In either case the anode plate, insert and orifice are all located concentric with the cathode centerline at a plane ~2 mm downstream of and parallel to the cathode orifice plate.

Typical tests were conducted by heating the contactor and simulator cathodes to temperatures where significant thermionic electron emission could occur (~1300 K), establishing high expellant (xenon) flowrates through them, and biasing their anodes positive using the discharge supplies to initiate cathode-to-anode discharges at each device. Next, the desired contactor and simulator flowrates ($\dot{m}_c$ and $\dot{m}_s$) and discharge current levels (J_{CD} and J_{SD}) were established; the contactor was biased relative to the simulator using the bias power supply; and voltage, current and probing instrument data were collected. The voltages and currents measured during typical tests are designated by the symbols shown within the circles in Fig. 2; they include the contactor and simulator discharge currents and voltages (J_{CD}, J_{SD}, V_{CD} and V_{SD}), the bias voltage between the contactor and simulator (V_B) and the contactor and simulator electron emission currents (J_{CE} and J_{SE}).

The two switches shown at the contactor and simulator in Fig. 2 are positioned at either the "EE" or "EC" position depending on whether the contactor is biased negative of the simulator and therefore Emitting Electrons (EE) or biased positive and therefore Collecting Electrons (EC). It is necessary to position these switches differently for each operating mode to assure that intentional limitations imposed on the discharge current levels (J_{CD} and J_{SD}) do not result in unintentional limitations being imposed on the electron emission or collection currents.[5]

The tank bias switch shown in Fig. 2 was installed so the vacuum tank could be allowed to float relative to the contactor/simulator system or be connected to the simulator or the contactor. Tests were conducted to investigate the effects of tank potential on contactor performance (contactor emission current vs. sheath voltage drop data) and on the plasmas produced around a contactor operating under various conditions. They showed a contactor collecting electrons exhibited essentially the same data suggestive of uniform current flow at the contactor whether the tank was floating or connected to the simulator cathode. Consequently, all electron collection data were acquired with the tank connected to the simulator cathode.

Data obtained with the contactor operating at a high electron emission current, on the other hand, suggested the current flow was concentrated along the tank centerline at high emission current levels unless the tank was at simulator anode potential. Such a condition was not considered representative of what would happen in space where the electrons would be free to go into an enveloping space environment rather than to a small simulator anode. Other data suggested that the most meaningful electron plasma property data associated with electron collection (i.e. those least perturbed by tank wall effects) were obtained with the tank either isolated or connected to the contactor cathode. Hence a compromise was made in obtaining data from a contactor emitting electrons. Contactor performance data which had to be gathered over a wide current range were obtained with the tank at simulator anode potential while plasma property data were obtained at a low emission current with the tank at contactor cathode potential.

The plasma environment produced between the contactor and the simulator was probed using the various instruments shown in Fig. 1. These instruments, the function they serve and the physical volume in which they can be used are:

Emissive Probe- This sensor and the associated circuitry system, which are similar to those used by Aston,[6] yield plasma potential data directly. The sensor can be swept axially downstream from the contactor to the simulator and/or radially along an arc that extends from the tank/contactor centerline out to a radius of approximately 30 cm. Probe output voltage (i.e. plasma potential) and position are recorded simultaneously on an X-Y plotter to assure well-correlated values of the data.

Langmuir Probe- The sensor used on this probe is a 3.2 mm dia. stainless steel sphere that can be moved conveniently into any position occupied by the emissive probe. Probe current/voltage characteristic curves recorded at these positions are analyzed using a two electron-group numerical model[7] that is assumed to describe plasmas such as these. This analysis yields the density and temperature of a Maxwellian electron group and the density and energy of a primary (or mono-energetic) electron group. This analysis is aided by inputting plasma potential data determined using the emissive probe at each location where Langmuir probe data are collected. The circuitry together with additional detail about the numerical procedures used to obtain plasma information have been described previously.[8]

Shultz-Phelps Ionization Gauge- This commercially available pressure gauge[9] was modified by removing the glass enclosure around the sensor so its spatial resolution would be improved. This probe was used to measure the pressure distributions over the same region swept by the emissive and Langmuir probes. Because gauge readouts from this device are inaccurate when a plasma is present, the measurements were made only when the plasma discharges were extinguished.

Retarding Potential Analyzer (RPA)- The sensor on this instrument was designed so it could be swept through an arc that passed through the tank centerline, was centered at the cathode orifice, and had a radius of about 18 cm. In the course of moving through this arc its aperture remained pointed at the cathode orifice as suggested in Fig. 1. Its purpose was to measure the current density of high energy ions that approached it from the contactor plume. As shown in Fig. 3, it consists of a cylindrical stainless steel Faraday cage ~13 mm in diameter with a 4 mm diameter orifice in one end of it. Ions that pass through this orifice are collected on a 9 mm diameter Molybdenum surface positioned ~3 mm downstream of the orifice plate. The data collected by the RPA was obtained when it was positioned in the ambient plasma region and oriented so that the orifice was facing the double-sheath. The Faraday cage surrounding the collector was biased 20 V below vacuum tank potential to prevent all electron (even high energy ones originating at the simulator cathode) from reaching the RPA collector. When the bias on the collector is varied relative to local plasma potential while

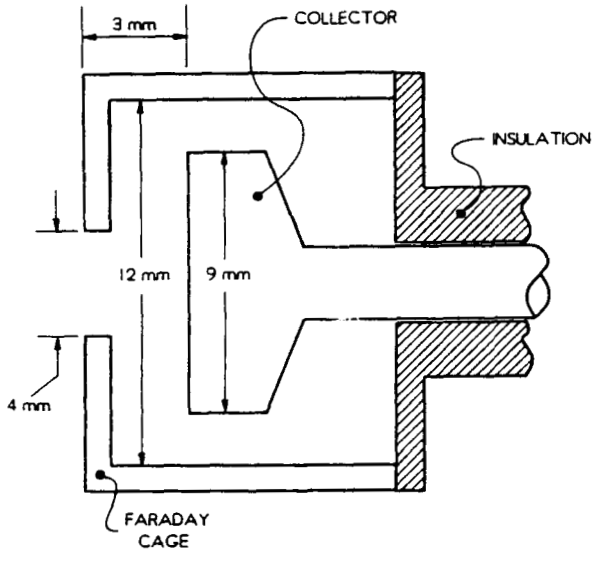

Fig. 3 Retarding Potential Analyzer

the device is pointed at a contactor collecting electrons ion current density (collector ion current/RPA aperture area) data like those shown in Fig. 4 are obtained.

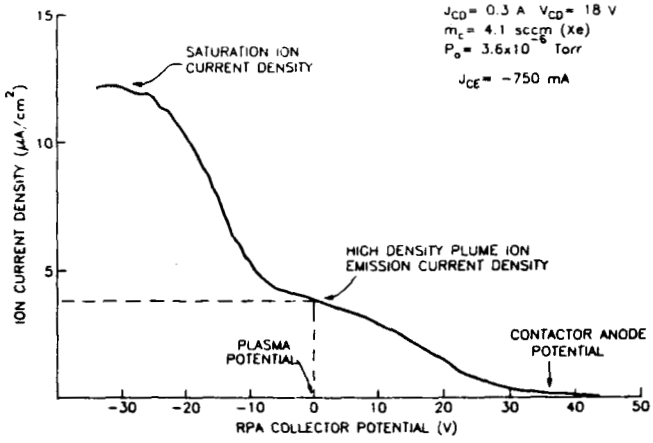

Fig. 4 Typical RPA Current Density/Potential Curve

When the collector is biased negative (< -25 V) the data of Fig. 4 indicate the collected current saturates. The magnitude of this current is determined by the fact that both ambient plasma ions and energetic ions streaming from the contactor are being collected. As the collector potential is increased above -25 V, the rate of ion collection from the ambient plasma ions drops off. As the potential is increased above 0 V ions accelerated from the contactor plume (plume ions) which have substantial energies but may not be reaching the collector surface with their full velocity normal to the surface begin to be repelled. Finally, the near-normal incidence plume ions are repelled from the collector as the current to it drops to zero at a potential near a value that corresponds to the maximum energy the ions should have (i.e. near contactor anode potential). There are several aspects of the probe design that cause it to behave in a non-ideal way[10], but it is believed that it yields reasonable plume ion current density data when the collector potential is greater than ambient plasma potential. In the present case the ion current density due to plume ions is defined somewhat arbitrarily as the value measured 2 V above plasma potential. As the data of Fig. 4 suggest, however, the value of plume current density is not particularly sensitive to the potential used as long as it lies within a few volts of this value.

Results

The overall performance of a hollow cathode plasma contactor tested under typical conditions in the experimental apparatus of Fig. 1 is shown in Fig. 5. This performance is presented as a plot of electron emission current versus contactor potential (i.e. the potential difference between the contactor and the ambient plasma with which it is exchanging current). The contactor was operated at the conditions listed in the legend and the tank bias switch was connected to the simulator. At potentials below -25 V the contactor is shown to emit electrons very easily (and most of this current is collected on the tank walls). On the other hand, at positive potentials, where the contactor is collecting electrons from the ambient plasma, the behavior is different. In fact, the contactor is shown to exhibit poor electron collection performance until a sufficiently high

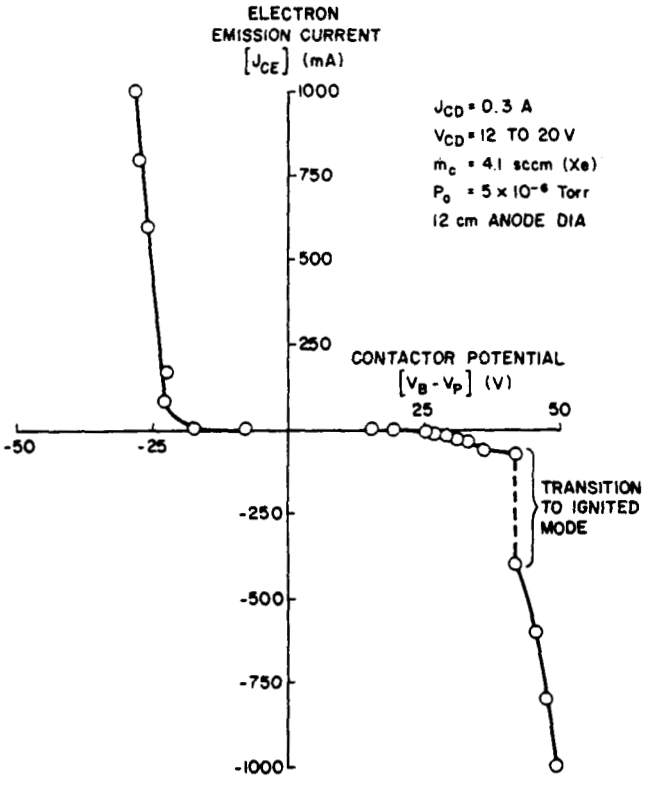

Fig. 5 Typical Plasma Contactor Performance Curve

potential is reached (~40 V in Fig. 5). At this potential the electron collection current increases quite suddenly. This sudden increase in current, identified as a "transition to ignited mode" operation has been linked to enhanced ionization of neutrals in the contactor anode plasma by electrons streaming through the double-sheath from the ambient plasma.[4]

Electron Collection Calibration Data

Extensive data have been collected using a contactor operating at one collection current, flowrate and discharge power condition so they can be used to calibrate numerical models of this process. This section will concentrate on describing the results obtained during such a test and indicating the extent to which these results agree with a simple physical model of the electron collection process.

The plasma potential structure that develops in the region surrounding a contactor collecting electrons is shown in Fig. 6. In this case the contactor is collecting 750 mA of electrons from the ambient plasma, and the sheath potential drop is about 32 V. It is operating at a relatively low discharge power of 5.4 W (the product of the discharge current (J_{CD}= 0.3 A) and voltage (V_{CD}= 18 V)). This power presumably goes into sustaining the plasmas within and outside of the contactor hollow cathode and maintaining the temperature of its insert at the value needed to sustain the desired discharge current (about 1300 K). The heater, shown in Fig. 2, is also used to sustain the insert temperature and was generally supplying 50 W of power. The flowrate of neutral xenon atoms through the contactor hollow cathode was at a typical value of 4.1 standard cubic centimeters per minute (sccm (Xe)) while that through the simulator was 3.4 sccm (Xe). These flowrates may also be expressed respectively as 280 and 230 milliamperes equivalent (mA eq)--flowrate expressed as the current of atoms that would flow if each carried the charge of 1.6x10^{-19} C. These flowrates induced a vacuum system background pressure of 3.6x10^{-6} Torr.

The plasma potential variation measured along the centerline of the contactor/vacuum tank at this operating condition is shown in Fig. 7. Also listed on this figure are the Maxwellian electron temperatures and plasma densities (densities due to both primary* and Maxwellian electron groups) measured in the contactor plume and ambient plasma regions. If one assumes that the electron collection current flowing from the ambient plasma to the downstream boundary of the double-sheath is determined by the ambient plasma random current density and the area of the downstream boundary (A_o), then this current can be expressed mathematically as

$$|J_{CE}| = \frac{1}{4} e\, n_{eo}\, A_o \sqrt{\frac{8\, k\, T_{eo}}{\pi\, m_e}}\ \beta\ . \quad (1)$$

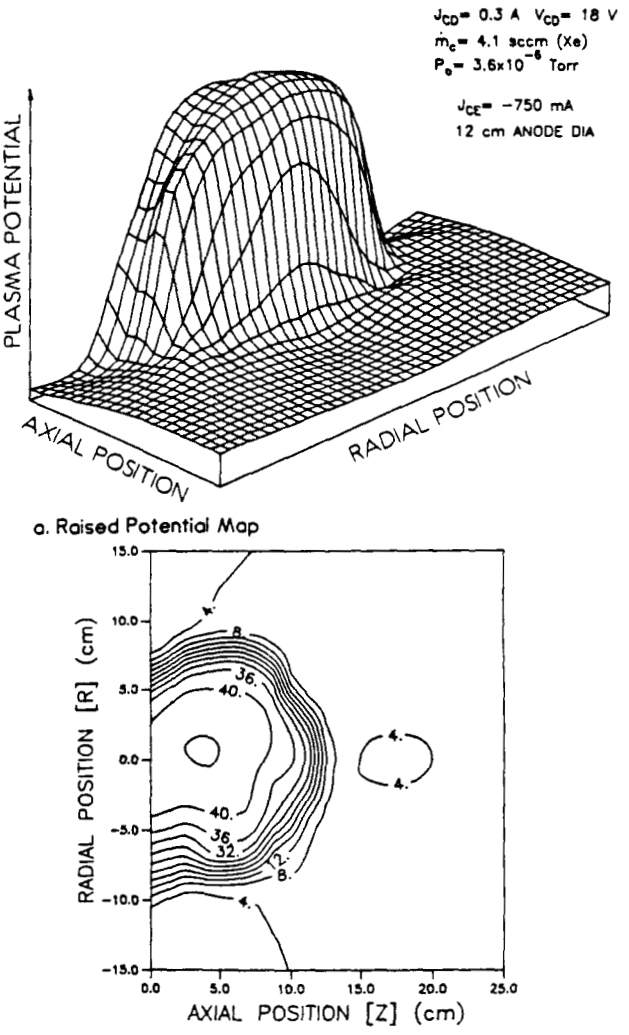

Fig. 6 Typical Plasma Potential Variation Near a Contactor Collecting Electrons

*The mono-energetic or primary electron group contributed densities of 1x10^{8} and 2.7x10^{6} cm^{-3} at energies of 45 eV and 52 eV in the contactor plume and ambient plasma regions, respectively.

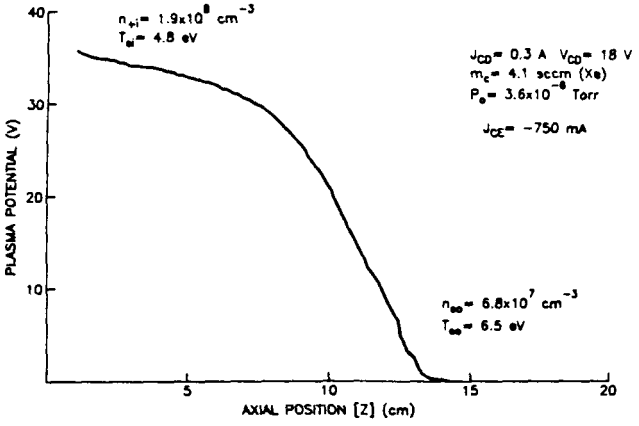

Fig. 7 Plasma Potential Variation Along the Contactor/Vacuum Chamber Centerline

In Eq. 1, e is the electronic charge, m_e is the electronic mass, n_{eo} and T_{eo} are the ambient plasma electron density and temperature, and k is Boltzmann's constant. The parameter β in Eq. 1 is a presheath factor that accounts for enhanced electron collection from the ambient plasma. It will be assumed to have a value of 1.49 in this study.[13] By measuring the area of the downstream boundary of the double-sheath (A_o) determined from the data in Fig. 6 to be 840 cm^2 and using the ambient plasma properties listed in Fig. 7, Eq. 1 can be used to estimate the electron collection current at $|J_{CE}|$ = 581 mA. This value is only 22% below the measured current of 750 mA and is considered to be within the range of experimental error.

A similar technique can be used to calculate the ion current which is being emitted from the contactor plume plasma to the upstream boundary of the double-sheath if one assumes that the contactor plume ions approach this boundary at the Bohm velocity.[11] The equation which expresses this current mathematically is

$$J_+ = e\, n_{+i}\, A_i \sqrt{\frac{k\, T_{ei}}{m_+}}\ \gamma. \qquad (2)$$

Using an upstream boundary area (A_i) of 360 cm^2 measured from the data presented in Fig. 6, the ion density (n_{+i} - the sum of the Maxwellian and primary densities) and Maxwellian electron temperature T_{ei} data presented in Fig. 7, the xenon ion mass (m_+) and a value of γ of 0.6;[11] one can compute the ion emission current from Eq. 2 to be 1.3 mA. If one assumes that both the electron and ion currents are flowing through the double-sheath region at the space-charge-limited condition, then the ion emission current can also be written as

$$J_+ = \sqrt{\frac{m_e}{m_+}}\ \frac{|J_{CE}|}{\alpha}. \qquad (3)$$

In Eq. 3, α is a non-dimensional parameter that depends on the geometry of the sheath, but which should be close to unity for the relatively thin sheath suggested by the data of Fig. 6. The ion emission current calculated using Eq. 3 is 1.5 mA, and this is close to the value found from Eq. 2 (1.3 mA).

In order to assure that sufficient excitation and ionization reactions are induced in the contactor plasma plume by electrons streaming into it from the ambient plasma, it is necessary to determine if the neutral atom density is sufficient to give a reasonable electron-atom inelastic collision frequency. The raised density and equal density contour maps of Fig. 8 show the axial and radial variation in xenon atom density measured immediately downstream of the contactor at the contactor ($\dot{m}_c$) and simulator ($\dot{m}_s$) flow conditions which induced the indicated ambient pressure (P_o). These data have been computed on the basis of pressure measurements by applying the perfect gas equation and assuming the background gas was in equilibrium with a 300 K vacuum chamber. Gas being ejected from the contactor was assumed to be at 1300 K (the estimated temperature of the hollow cathode). The data of Fig. 8 suggest the density drops from a high value at the contactor orifice to background levels at distances several centimeters from it.

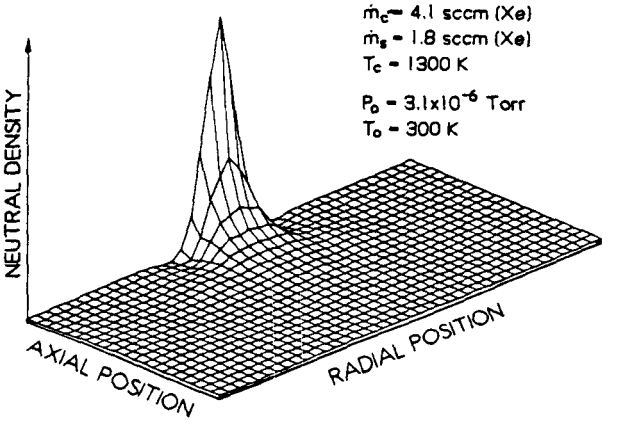

a. Raised Neutral Density Map

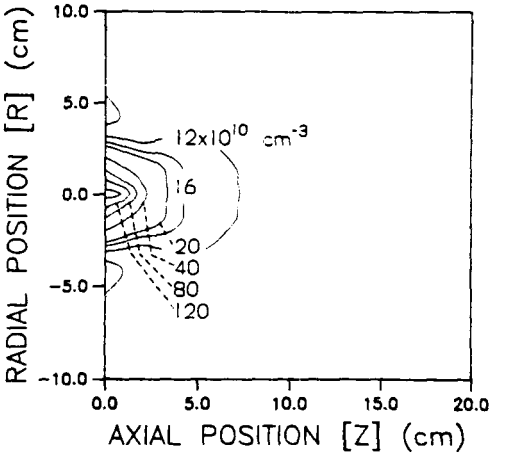

b. Equi-density Contour Map

Fig. 8 Variation in Neutral Atom Density near the Contactor

Using data like those shown in Fig. 8, typical ion production rates due to electrons streaming toward the contactor cathode can be computed.[4] Results obtained from such calculations are shown in Fig. 9 in the form of a plot of integrated ion production rate by electrons that have streamed from the inner radius of the double-sheath to the radius values indicated on the horizontal axis. In order to make this calculation it has been assumed that the electrons are streaming uniformly on radial inward trajectories toward the contactor orifice and the neutral atoms supplied at the contactor orifice are streaming radially outward.

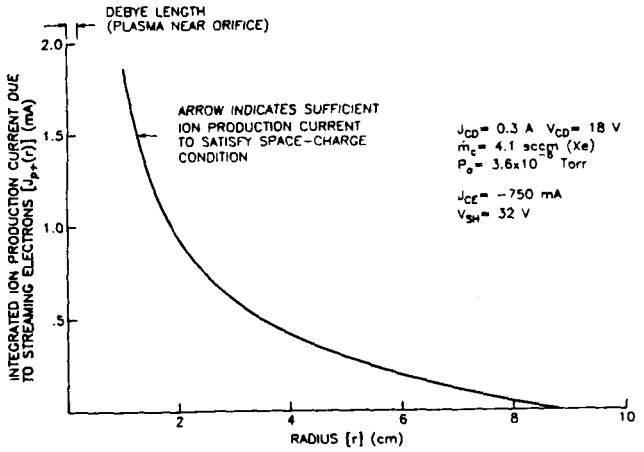

Fig. 9 Simple Spherical Model Prediction of Ion Production by Streaming Electrons

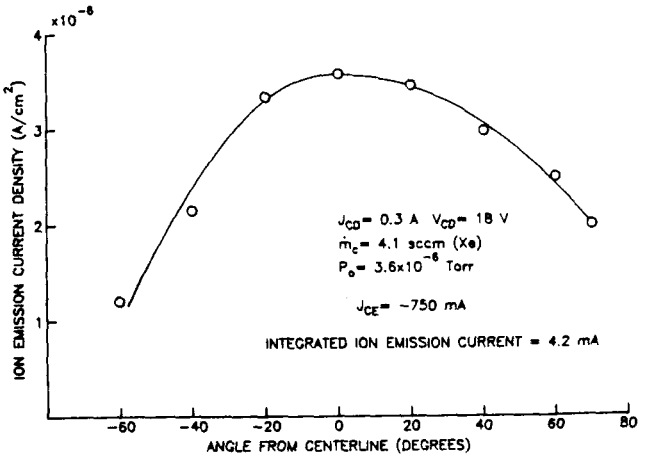

Fig. 10 Azimuthal Variation of Current Density of Ions Emitted from the Contactor Plasma

The calculations have been made for the operating point associated with Figs. 6, 7, and 8. The curve indicates that the ion production rate increases dramatically as the streaming electrons approach the contactor orifice ($r \rightarrow 0$) because the xenon density is highest there. The location of the arrow on the curve (at 1.3 cm) indicates the radial position where the ion production due to streaming electrons alone would be sufficient to satisfy the space-charge-limited ion current required at the electron current being collected (J_{CE} = -750 mA). Hence it is suggested that ion production induced by streaming electrons could be sufficient to assure low voltage operation of a contactor collecting electrons without including any ions produced in the hollow cathode-to-anode discharge. It is noted in this regard that discharge-produced ions are generated sufficiently close to the cathode so they can recombine on hollow cathode or anode surfaces more readily than ions produced by streaming electrons. It is considered likely that essentially all ions produced within a few Debye shielding lengths of the cathode (identified in Fig. 9) by either mechanism would be lost to the cathode. It is considered to be particularly noteworthy that the discharge current (J_{CD}) may be reduced to zero without inducing a change in the sheath voltage drop once the contactor is collecting electrons stably in the ignited mode. This observation also supports the hypothesis of substantial ion production by streaming electrons and is in agreement with observations made by Gilchrist et. al. in a tethered mother-daughter space experiment[12].

The retarding potential analyzer (RPA) described previously was used to measure the azimuthal profile of the current density of ions expelled across the double-sheath under the conditions associated with Figs. 6 to 9. The resulting data are shown in Fig. 10. Note that the ion emission current density is a maximum on the centerline and that it drops to lower values on either side of the centerline. One can integrate the ion emission current density data contained in Fig. 10 over a hemispherical surface with the radius of the RPA sweep arc (18 cm) to determine the overall ion emission current flowing from the contactor to the ambient plasma. The result of so doing is 4.2 mA in this case. Applying Eq. 3 to determine the space-charge-limited value of this current at the prevailing operating conditions one computes an ion emission current (1.5 mA) that is approximately one third of the measured value. Considering the uncertainties associated with these measurements and the space-charge limited model being applied, this is considered to be acceptable agreement.

Examination of Eq. 3, which is based on the assumption of space-charge-limited current flow through a double-sheath, suggests that the ion emission current should vary linearly with electron collection current. In order to demonstrate the validity of this equation and therefore the fact that a space-charge-limited double-sheath develops, the ion emission current density was measured on the centerline (a readily measured quantity that is proportional to J_+) as a function of the electron current being collected by the contactor. The data that were collected in this test are shown in Fig. 11. This graph displays the expected linear variation of ion current density versus electron current and is in agreement with Eq. 3, except for the fact that the slope of the line (1/250) is about twice the square root of the electron-to-xenon ion mass ratio (1/490). This difference could be explained by the geometrical differences between the actual shape of the double-sheath and the simple model of the process reflected in Eq. 3.

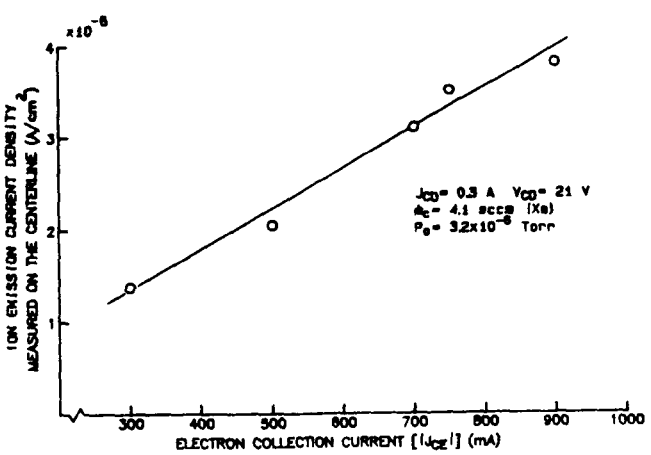

Fig. 11 Validation of Space-Charge-Limited Current Flow Assumption

One can change the size and geometrical conditions of the double-sheath by changing the flowrate to the contactor. This can be done because large flowrates tend to expand the contactor plume thereby increasing the ratio of the inner-to-outer dimensions of the double-sheath and

causing the potential difference across the double-sheath to decrease. Equation 3 suggests, however, that the ion emission current of a contactor should depend to first order only on electron collection current (and not on flowrate or sheath voltage drop). In order to demonstrate the validity of Eq. 3 more completely, a test was conducted in which the contactor flowrate was varied while the contactor electron collection current was held constant. The resulting data, showing ion emission current density on the centerline (which is proportional to the total ion emission current), are plotted against contactor flowrate in Fig. 12. This figure indicates that the ion emission current density remains relatively constant over the range of flowrates investigated. It is noted that the sheath potential drop for the data shown in Fig. 12 ranged from 66 V at a flowrate of 2.9 sccm (Xe) to 24 V at 6.3 sccm (Xe). This result is reasonable because the higher sheath potential drop is required at the lower flowrate to sustain the ion production rate by streaming electrons in an environment of lower neutral atom density within the contactor plume. The fact that the data of Fig. 12 show excellent agreement with Eq. 3 suggests that the difference between the slope of the line in Fig. 11 and the value of this slope predicted by Eq. 3 cannot be completely explained on the basis of geometrical considerations.

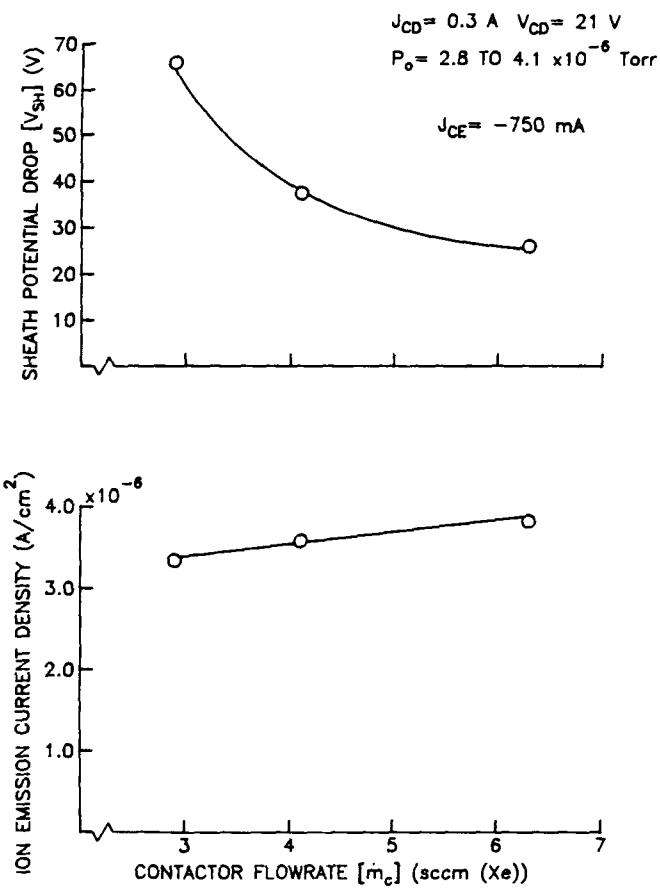

Fig. 12 Effects of Flowrate on Ion Emission Current Density at a given Electron Collection Current Condition

Effects of Anode Area on Electron Collection

Typical plasma property data measured downstream of a contactor operating with a 3 cm diameter anode (rather than the 12 cm diameter anode used in the tests that produced the data of Figs. 5 through 12) are shown in Figs. 13 and 14. Figure 13 contains potential maps in the region of the contactor measured at operating conditions that are similar to those obtained using the 12 cm diameter anode. The electron collection current is 250 mA in this case whereas 750 mA was being

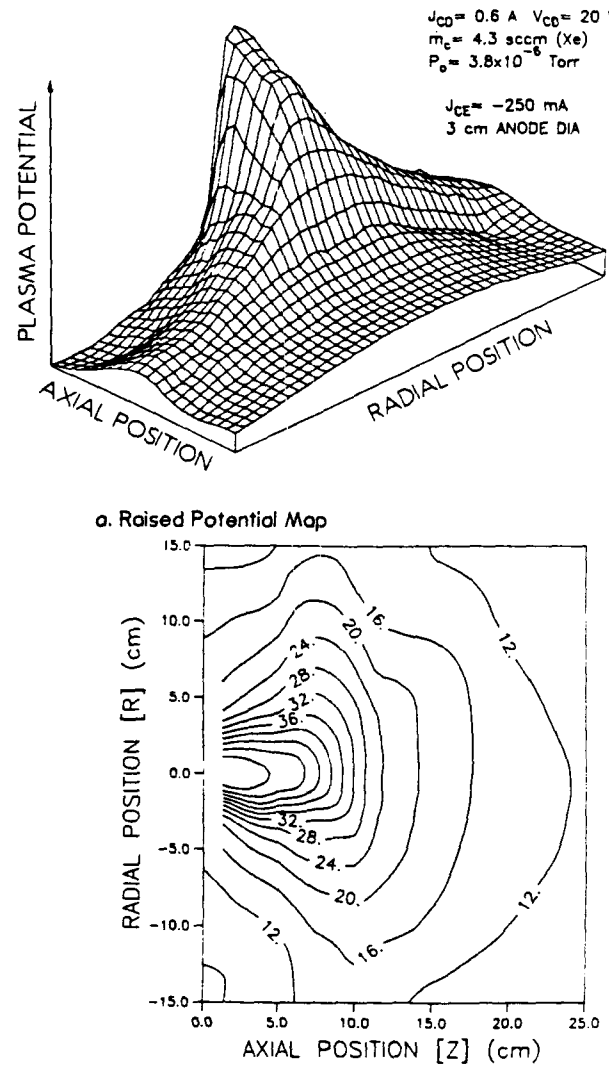

Fig. 13 Typical Plasma Potential Variation near a 3 cm Anode Diameter Contactor Collecting Electrons

collected with the 12 cm diameter anode. The most striking differences between the data of Figs. 13 and 6 are the higher voltage levels, the spreading of the double-sheath and the reduction in the size of the contactor plume when the smaller anode is used. Although the relative position, magnitude and shape of the equipotential contours are different, it is argued that the voltage difference that exists is being sustained by acceleration of counterflowing ion and electron currents in both cases. Thus the potential structure associated with both anodes reflects the double-sheath phenomenon. The differences appear to develop because the inner boundary of this double-sheath must remain anchored to and therefore have a dimension that is about equal to the associated anode diameter. This is a predictable result since the electrons would generally be collected on the anode.

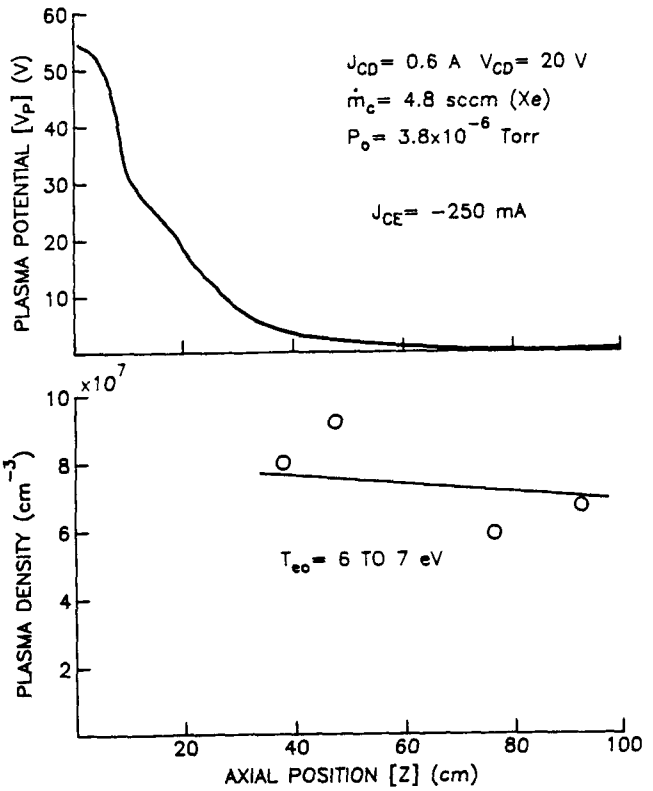

Fig. 14 Variation of Plasma Potential and Density along the Contactor/Vacuum Chamber Centerline (3 cm Anode Diameter Contactor)

The irregular shape of the double-sheath associated with the small anode (Fig. 13) makes it unsuitable for analysis using the simple, spherical model of Ref. 4. It is expected, however, that the smaller anode case can be modelled numerically. It is noted that the potential structure shown in Fig. 13 is similar to those reported by Patterson and Aadland[13] for tests involving electron collection from what appears to have been a rather low ambient density plasma at current levels above 1 A on a contactor that utilized a 24 cm diameter anode. A review of their data together with data obtained by the authors (including that of Fig. 13) suggests a double-sheath takes on an irregular (non-spherical) shape when the downstream boundary of the double-sheath becomes much larger than the anode diameter.

The plasma properties, measured downstream of the contactor with the 3 cm diameter anode, along the centerline of the vacuum tank, are shown in Fig. 14. The top plot in Fig. 14 displays the plasma potential variation and the bottom one shows the plasma density variation as functions of axial position. The plasma density data are only shown beyond 40 cm because the strong potential variation that exists upstream of that position generally makes the associated Langmuir probe trace aquisition and analysis unreliable. The analysis of the Langmuir probe traces obtained downstream of the 40 cm position indicate that the ambient plasma* contained mostly Maxwellian electrons with a temperature of 6 to 7 eV and a density of about 8x10^7 cm^{-3}. It was possible to obtain one Langmuir probe trace close to the contactor (i.e. 2 cm downstream of the anode) and it indicated that two electron groups were present, a Maxwellian group with a temperature of about 5 eV and a density of 2.4x10^9 cm^{-3} and a primary group with an energy of ~57 eV and a density of 3x10^8 cm^{-3}. It is suggested that this primary group consists of electrons that have been accelerated from the ambient plasma and have suffered no energy-degrading collisions. These data are not included in the bottom plot of Fig. 14 since data from only one position were collected and no trends could be inferred. Note, however, that the plasma density in the region close to the contactor is about 3 times that in the ambient plasma. This result is also consistent with results obtained using contactors with larger anode diameters.

*Although the Langmuir data did not fit the assumed distribution model perfectly, analysis indicated that the ambient plasma also consisted of ~1x10^7 cm^{-3} of primary electrons with an energy of 30 to 40 eV

Electron Emission

The plasma potential variation downstream of a typical contactor which is emitting electrons is shown in Fig. 15. The contactor cathode (at the 0,0 location) is at the lowest potential (-17 V) of any point in the maps. Downstream of that point the potential rises to a ridge along which the potential peaks before it drops off and levels out. The peaked potential structure is noteworthy and

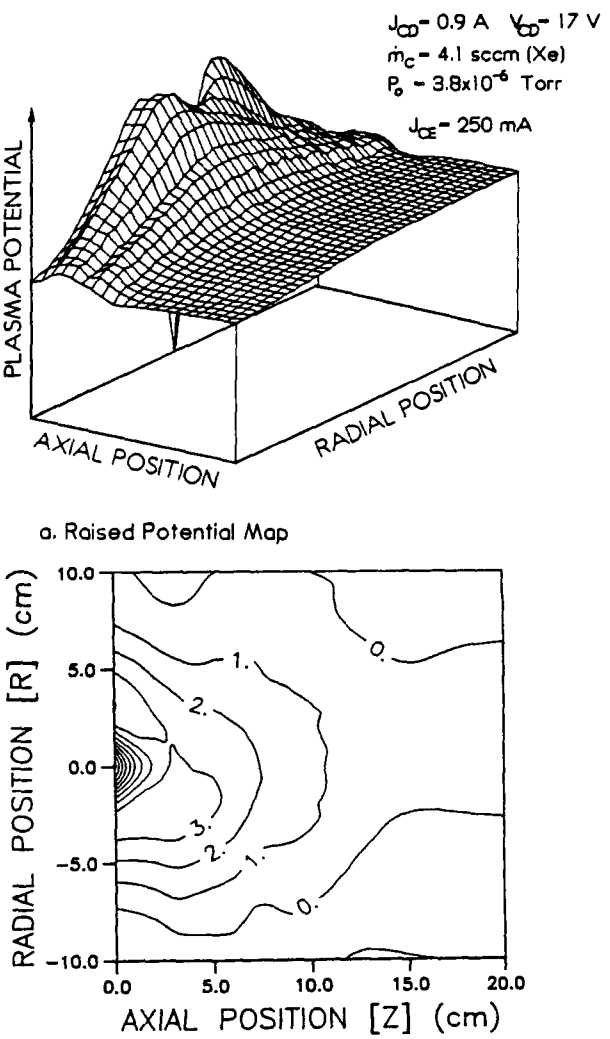

Fig. 15 Typical Plasma Potential Structure Occurring near a Contactor Emitting Electrons

was initially unexpected. Figure 16 shows this structure in a series of plasma potential profiles measured along the centerline between the contactor (emitting electrons) and the simulator (collecting electrons) at different electron emission currents. These curves were measured using an emissive probe with the contactor operating at the conditions listed in the legend. They were obtained with the tank bias switch connected to the contactor (see Fig. 2) and the plasma potentials shown are measured with respect to contactor cathode potential. These profiles show a potential hump near (within 1 cm of) the contactor that becomes increasingly larger as the emission current is reduced.

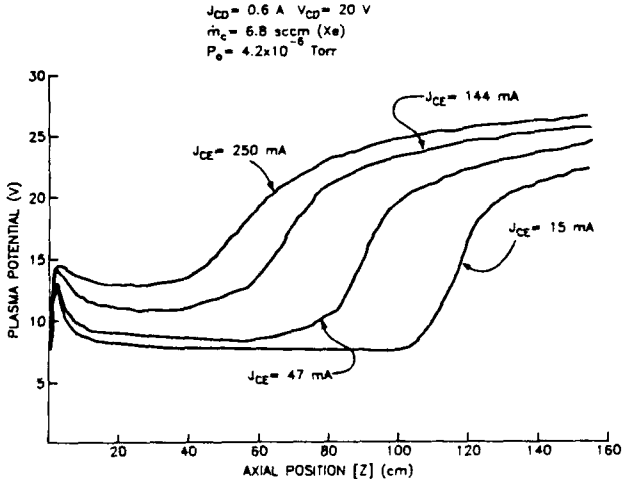

Fig. 16 Effects of Electron Emission Current on Plasma Potential Profiles

The mechanism by which the potential structures shown in Figs. 15 and 16 are believed to be produced can be understood by considering the simplified schematic and corresponding potential profile shown in Fig. 17. In the potential environment shown, electrons emitted from the cathode would be accelerated through the potential gradient at the contactor to the point where they had sufficient kinetic energy to enable them to excite and ionize neutral atoms that are present at a high density near the contactor. It is the associated ion production that would be expected to produce the overabundance of ions that causes the potential humps shown in Figs. 15 and 16 to develop. This ion overabundance is expected because electron kinetic energy which would typically exceed the energy needed for ionization would tend to cause the less massive electrons to leave the region of ionization more rapidly than the ions.[15] Immediately downstream of the peak potential the potential drops and forces develop that decelerate the electrons and accelerate the ions. The region downstream of the potential hump is one in which the measurements show ion and electron densities are relatively low, the electrons are mono-energetic and the required net electron current is being conducted via a plasma expansion process to the surrounding ambient plasma. This result is similar to that predicted by the model of Davis et. al.[16] except for the fact that this model is based on the assumption of Maxwellian electrons expanding in accordance with the barometric equation rather than mono-energetic electrons.

Langmuir probe data collected throughout the regions identified in Fig. 17 suggest that the

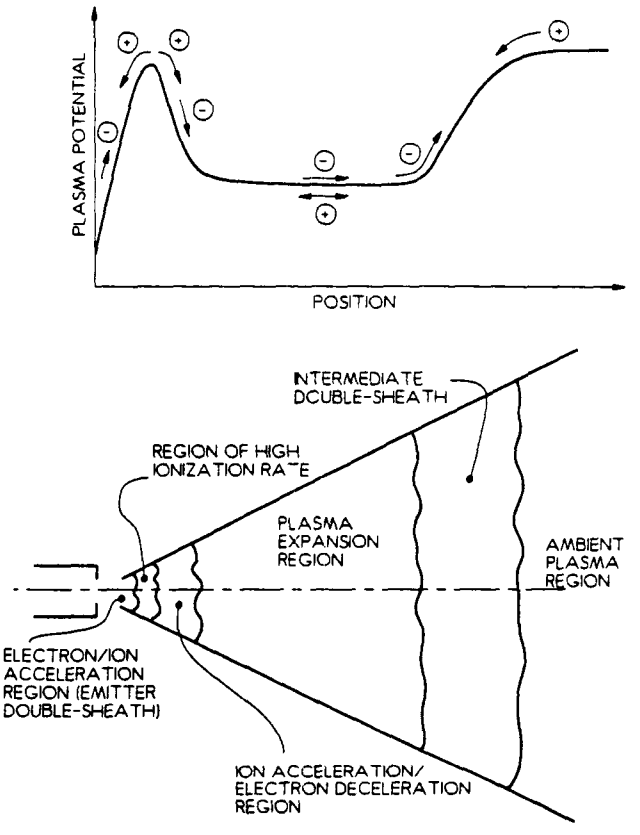

Fig. 17 Simple Physical Model of Electron Emission Process which Occurs within the Vacuum Chamber

electron current being emitted from the contactor hump expands in a spherically symmetric manner up to the point where the plasma potential begins to rise again. The sheath structure associated with this rise is typically located 40 to 100 cm downstream of the contactor and exhibits a potential rise of ~10 V. It serves as a boundary between the spherically expanding plasma coming from the contactor and the ambient plasma which fills the majority of the vacuum chamber. The location of this boundary could very well be determined by the interaction of the intermediate double-sheath and the vacuum tank wall. Whether or not this is the case has not been verified, but it is noted that the existence of the sheath is not influenced by switching the tank between contactor cathode and floating potentials. On the other hand, connecting the tank to the simulator anode causes the potential structure shown in Figs. 15 through 17 to disappear.

The ambient plasma downstream of the intermediate double-sheath shown in Fig. 17 has a higher plasma density than the region of spherical expansion plasma nearest it. The ambient plasma contains mostly Maxwellian electrons with a temperature of 5 to 7 eV. Obviously, the electrons drawn from the contactor sustain the ambient plasma by producing ions, but the reason why a distinct boundary develops between the expansion and ambient plasma regions is not understood. The work conducted to date has not focused on the structure of the second sheath, the processes associated with sustaining it, or parameters which might influence its characteristics. It has instead addressed the plasma expansion processes occurring between the contactor and a position approximately 40 cm downstream of it.

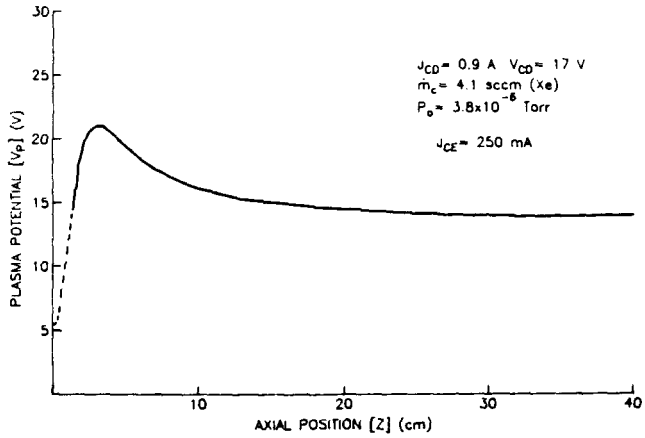

Fig. 18 Plasma Potential Profile Measured in the Plasma Expansion Region

The typical plasma potential profile shown in Fig. 18 was measured at slightly different operating conditions than the ones listed in Fig. 16. The dotted section of the curve was drawn after the data were taken and is meant to suggest that the plasma from which the 250 mA of electron current is being extracted is at a potential of ~6 V. This value of potential was found by measuring the energy of the electron population in the region downstream of the contactor and by assuming that many of the mono-energetic electrons found in the plasma expansion region have not suffered energy-degrading collisions as they have expanded away from the contactor.

Spherical expansion of a plasma containing electrons of kinetic energy E and velocities directed radially outward from their source point can be described in terms of the current flowing by the equation

$$J_{CE} = e\, n_e\, \psi\, r^2 \sqrt{\frac{2\, e\, E}{m_e}} \quad . \quad (4)$$

In Eq. 4, n_e is the density of emitted electrons at a radius r measured from the source point and ψ is the solid angle through which the electrons are expanding. At the fixed emission current, this equation shows the associated electron density should vary inversely with the square of the radius r and the square-root of the energy E.

Experimental measurements of the variation in Langmuir probe electron current at plasma potential (which is proportional to the electron density-velocity product) have been made as a function of distance from the contactor cathode at the operating conditions associated with the data of Fig. 18. These data are shown in the form of a plot of probe current versus position on a log-log scale in Fig. 19. The fact that this plot is linear and has a slope of -2 indicates that the expected $1/r^2$ variation of electron density is observed and that the spherical expansion model of the process is appropriate. In addition, the intercept shown on the figure can be used to estimate the solid angle ψ through which the electrons are expanding. For the data of Fig. 19, calculations indicate this angle should be slightly greater than 3.5 steradians (~one-forth of a full sphere).

Conclusions

A detailed study of a contactor collecting electrons conducted with an anode that produced a

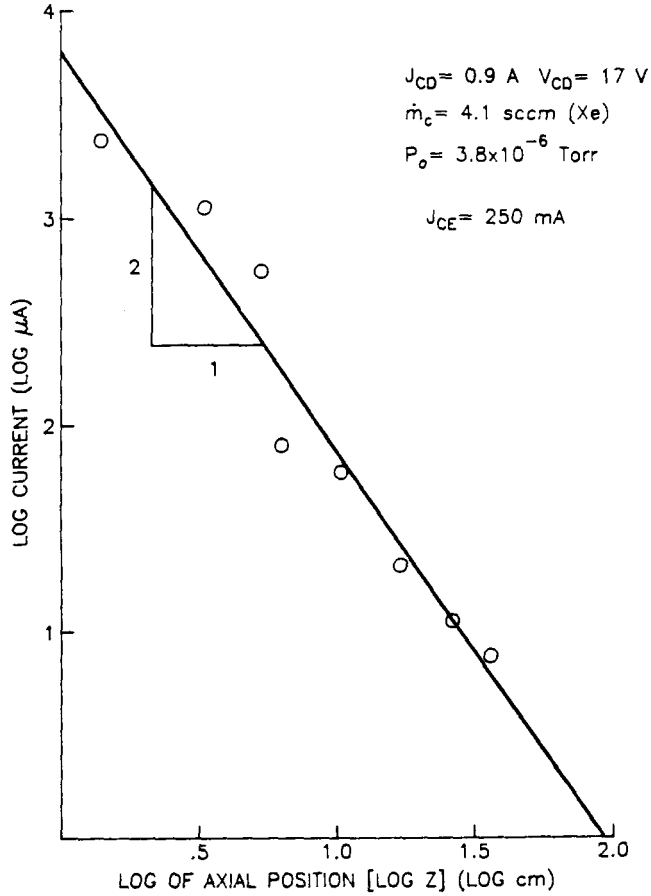

Fig. 19 Probe Current Versus Position Data Measured in the Plasma Expansion Region

nearly hemispherical double-sheath shows good agreement and is self-consistent with a simple one-dimensional spherical model. Data collected using a contactor with a smaller anode show substantial distortion from the spherically shaped double-sheath and consequently the elementary spherical model cannot be applied to it. Based on these and data reported by other investigators[14] it is suggested that the elementary model begins to break down when the diameter of the downstream boundary of the double-sheath exceeds (by a factor of 3 to 4) the diameter of the planar contactor anode on which electrons are collected. In all cases, results suggest the same physical phenomena related to the development of a double-sheath and ionization by electrons streaming across this sheath toward the contactor appear to be active. The detailed data obtained using both the large and small anode contactors should prove to be useful in developing and calibrating more elaborate models suitable for use in predicting contactor performance over wide ranges of operating conditions.

In the electron emission mode development of a region of high ion production close to the cathode orifice followed by a region of rapid potential dropoff is observed. This region is followed in turn by a region of constant potential in which mono-energetic electrons stream toward a simulated ambient plasma in a spherically symmetric manner. Present instrumentation is not adequate to verify this physical model of the region under all operating conditions and more experimental work is necessary to identify other important phenomena.

References

1. Purvis, C.K., and R.O. Bartlett, "Active Control of Spacecraft Charging," Progress in Astron. Aeron., H.B. Garrett and C.P. Pike, eds., V. 71, 1980, pp. 299-317.

2. Martinez-Sanchez, M. and D.E. Hastings, "A Systems Study of a 100 kW Tether," appears in "Tethers in Space," P. Bainum, I. Bekey, L. Guerriero, P. Penzo, eds., Advances in the Astronautical Sciences, V. 62, 1987.

3. Williams, J.D. and P.J. Wilbur, "Plasma Contacting - An Enabling Technology," AIAA Paper No. 89-0677, 9-12 January 1989.

4. Williams, J.D., P.J. Wilbur, and J.M. Monheiser, "Experimental Validation of a Phenomenological Model of the Plasma Contacting Process," appears in "Space Tethers for Science in the Space Station Era," L. Guerriero and I. Bekey, eds., Societa Italiana Di Fisica, V. 14, Venice, Italy, 4-8 October 1987.

5. Williams, J.D., "Electrodynamic Tether Plasma Contactor Research," appears in "Advanced Electric Propulsion and Space Plasma Contactor Research," P. Wilbur, ed., NASA CR-180862, Jan. 1987, pp. 1-75.

6. Aston, G. and P.J. Wilbur, "Ion Extraction from a Plasma," J. Appl. Phys., V. 52, No. 4, April 1981, pp. 2614-2626.

7. Beattie, J.R., "Numerical Procedure for Analyzing Langmuir Probe Data," AIAA Journal, V. 13, No. 7, July 1975, pp. 950-952.

8. Laupa, T., "Thick Sheath Langmuir Probe Trace Analysis," appears in "Advanced Electric Propulsion and Space Plasma Contactor Research," P. Wilbur, ed., NASA CR-175119, Jan. 1986, pp. 128-138.

9. Anonymous, "Instruction Manual No. 0-01-224017 for Ionization Gauge Controllers," Granville-Phillips Co., Boulder, CO, USA, 1971.

10. Boyd, R.L.F., "The Collection of Positive Ions by a Probe in an Electrical Discharge," Proc. Roy.Soc., V. 201A, 1950, pp. 329-347.

11. Bohm, D.E., "Minimum Ionic Kinetic Energy for a Stable Sheath," appears in The Characteristics of Electrical Discharges in Magnetic Fields, A. Guthrie and R.K. Wakerling, eds., McGraw-Hill Book Co., New York, 1949, pp. 77-86.

12. Gilchrist, B.E. and et.al. "Electron Collection Enhancement Arising from Neutral Gas Jets On a Charged Vehicle in the Ionosphere," to be published in Journal of Geophysical Research.

13. Katz, I. and V.A. Davis, "On the Need for Space Tests of Plasma Contactors as Electron Collectors," appears in "Space Tethers for Science in the Space Station Era," L. Guerriero and I. Bekey, eds., Societa Italiana Di Fisica, V. 14, Venice, Italy, 4-8 October 1987.

14. Patterson, M.J. and Randall S. Aadland,"Ground-Based Plasma Contactor Characterization," appears in "Space Tethers for Science in the Space Station Era," L. Guerriero and I. Bekey, eds., Societa Italiana Di Fisica, V. 14, Venice, Italy, 4-8 October 1987.

15. Langmuir, I., "The Interaction of Electron and Positive Ion Space Charges in Cathode Sheaths," Phys. Rev., V. 33, No. 6, June 1929, p. 954-989.

16. Davis, V., I. Katz, M. Mandell, and D. Parks, "Three Dimensional Simulation of the Operation of a Hollow Cathode Electron Emitter on the Shuttle Orbiter," appears in "Tethers in Space," P. Bainum, I. Bekey, L. Guerriero, P. Penzo, eds., Advances in the Astronautical Sciences, V. 62, 1987.

DISTRIBUTION LIST

	Copies
National Aeronautics and Space Administration Washington, DC 20546 Attn:	
Mr. Edward J. Brazill, Code MD	1
Mr. Thomas D. Stuart, Code MK	1
Dr. Stanley Shawhan, Code ES	1
Dr. L.R. Owen Storey, Code ES	1
Mr. George Levine, Code MTF	1
Mr. Ivan Bekey, Code Z	1
Mr. John L. Anderson, Code RS	1
National Aeronautics and Space Administration Lewis Research Center 21000 Brookpark Road Cleveland, OH 44135 Attn:	
Technology Utilization Office, MS 7-3	1
Report Control Office, MS 60-1	1
Library, MS 60-3	2
Dr. M. Goldstein, Chief Scientist, MS 5-9	1
Mr. Dave Byers, MS 500-219	1
Mr. Vincent Rawlin, MS 500-220	1
Dr. Carolyn Purvis, MS 302-1	1
Mr. Joseph C. Kolecki, MS 501-6	1
Mr. Michael Patterson, MS 500-220	1
Mr. Joel Galofaro, MS 302-1	1
Dr. Dale Ferguson, MS 302-1	10
National Aeronautics and Space Administration Lyndon B. Johnson Space Center Houston, TX 77058 Attn:	
Dr. James E. McCoy, Mail Code SN3	1
National Aeronautics and Space Administration Marshall Space Flight Center Huntsville, AL 35812 Attn:	
Mr. J. H. Laue, Mail Code FA31	1
Mr. Chris Rupp, Mail Code PS04	1
Mr. James K. Harrison, Mail Code PS04	1
NASA Scientific and Technical Information Facility P.O. Box 8757 Baltimore, MD 21240 Attn:	
Accessioning Dept.	1

	Copies
Dept. of the Navy Office of Naval Research Universiy of New Mexico Bandolier Hall West Albuquerque, NM 87131 Attn:	
G. Max Irving	1
Procurement Executive, Ministry of Defense Royal Aircraft Extablishment Farnborough, Hants GU14 6TD ENGLAND Attn:	
Dr. D. G. Fearn	1
United Kingdom Atomic Energy Authority Culham Laboratory Abingdon, Oxfordshire OX143DB ENGLAND Attn:	
Dr. A. R. Martin (Rm F4/135)	1
Defense Nuclear Agency DNA/RAEV Washington, D.C. 20305-1000 Attn:	
Captain Daniel Allred	1
SRT Technologies 1500 Wilson Blvd, Suite 800 Arlington, VA 22209-2415 Attn:	
Ms. Kaye Anderson	1
Air Force Astronautics Lab Edwards AFB, CA 93523 Attn:	
LKDH/Lt. Robert D. Meya, MS 24	1
LKDH/Lt. Phil Roberts, MS 24	1
Jet Propulsion Laboratory 4800 Oak Grove Laboratory Pasadena, CA 91109 Attn:	
Technical Library	1
Dr. Paul Penzo, Code 1156-217	1
Dr. Stephen Gabriel	1
TRW Inc. TRW Systems One Space Park Redondo Beach, CA 90278 Attn:	
Mr. Neal Holkower	1
Dr. Rob Stillwell	1

	Copies
National Aeronautics and Space Administration Ames Research Center Moffett Field, CA 94035 Attn:	
Technical Library	1
National Aeronautics and Space Administration Langley Research Center Langley Field Station Hampton, VA 23365 Attn:	
Technical Library	1
Mr. George Wood, Mail Code 234	1
Hughes Research Laboratories 3011 Malibu Canyon Road Malibu, CA 90265 Attn:	
Dr. Jay Hyman, MS RL 57	1
Dr. J. R. Beattie, MS RL 57	1
Dr. J. N. Matossian, MS RL 57	1
Rocket Research Co. P.O. Box 97009 Redmond, WA 98073-9709 Attn:	
Mr. William W. Smith	1
Mr. Paul Lichon	1
Mr. Lee Parker 252 Lexington Road Concord, MA 01741	1
Department of Aeronautics and Astronautics Massachusetts Institute of Technology Cambridge, MA 02139 Attn:	
Dr. Daniel E. Hastings, Rm 37-441	1
Institute for Space and Aeronautical Science 4-6-1 Komaba, Meguro-ku, Tokyo, 153, JAPAN Attn:	
Prof. K. Kuriki	1
Prof. T. Obayashi	1
Tokai University Kitakauame, Hiratsuka, Kanagawa, JAPAN Attn:	
Prof. K. Hirao	1

	Copies
Physics Department Naval Postgraduate School Monterey, CA 93943-5000 Attn:	
Dr. Chris Olson, Mail Code 61-OS	1
Martin Marietta Aerospace P. O. Box 179 Denver, CO 80201	1
Attn:	
Dr. Kevin Rudolph, MS MO482	1
S-Cubed P. O. Box 1620 LaJolla, CA 92038	1
Attn:	
Dr. Ira Katz	1
Dr. Victoria Davis	1
Electric Propulsion Laboratory, Inc. 43423 N. Division St., Suite 205 Lancaster, CA 93535	
Attn:	
Dr. Graeme Aston	1
Dr. John R. Brophy	1
Mr. Joe Carroll Energy Science Laboratories 11404 Sorrento Valley Rd., #112 San Diego, CA 92121	1
Instituto du Fisica dello Spazio Interplanetario Consiglio Nazionale dello Richerche Via G. Galilei 00044 Frascati, ITALY	
Attn:	
Dr. Marino Dobrowolny	1
Dr. Carlo Bonifazi	1
Dr. Luciano Iess	1
Mr. Giuliano Vannaroni	1
Science Applications International Corp. 13400 B Northrop Way #36 Bellevue, WA 98005	
Attn:	
Dr. Hugh Anderson	1
Starlab/SEL Stanford University Stanford, CA 94305	
Attn:	
Dr. Peter Banks	1
Dr. Roger Williamson	1

	Copies
Science Applications International Corp. Plasma Physics Division 1710 Goodridge Drive McLean, VA 22102 Attn: Mr. Edward P. Szuszczewicz	1
University of Alabama (Huntsville) Electrical and Computer Engineering Dept. Engineering Building Huntsville, AL 35899 Attn: Dr. Michael Greene	1
Physics Department Utah State University Logan, Utah 84322 Attn: Dr. W.J. Raitt	1